INSTITUTO POTOSINO DE INVESTIGACIÓN CIENTÍFICA Y TECNOLÓGICA, A.C.

POSGRADO EN CIENCIAS EN BIOLOGIA MOLECULAR

Synthesis and Electrophysiological Evaluation of 6,11-Dihydrodibenzo[c,f][1,2,5]thiadiazepine-5,5-dioxide (DBTD): Non-Competitive $GABA_A$ Receptor Antagonists

Tesis que presenta

Juan Francisco Ramírez Martínez

Para obtener el grado de

Doctor en Ciencias en Biología Molecular

Director de la Tesis:

Dr. Carlos Barajas López

San Luis Potosí, S.L.P., Enero de 2013

Constancia de aprobación de la tesis

La tesis **"Synthesis and Electrophysiological Evaluation of 6,11-Dihydrodibenzo[c,f][1,2,5]thiadiazepine-5,5-dioxide (DBTD): Non-Competitive $GABA_A$ Receptor Antagonists"** presentada para obtener el Grado de Doctor en Ciencias en Biología Molecular fue elaborada por **Juan Francisco Ramírez Martínez** y aprobada el **16 de Enero de 2013** por los suscritos, designados por el Colegio de Profesores de la División de Biología Molecular del Instituto Potosino de Investigación Científica y Tecnológica, A.C.

Dr. Roberto Martínez

Asesor externo

Dra. Marcela Miranda Morales

Asesor externo

Dr. Carlos Barajas López

Director

Dr. Marco M. González Chávez

Asesor externo

Dr. Rubén López Revilla

Asesor interno

Créditos Institucionales

Esta tesis fue elaborada en el Laboratorio de Laboratorio de Neurobiología de la División de Biología Molecular del Instituto Potosino de Investigación Científica y Tecnológica, A.C., bajo la dirección del Dr. Carlos Barajas López.

La parte de síntesis y de cálculos teóricos fue realizada en el Laboratorio de Síntesis Orgánica del Centro de Investigación y Estudios de Posgrado, Facultad de Ciencias Químicas de la Universidad Autónoma de San Luis Potosí, bajo la dirección del Dr. Marco Martín González Chávez.

Durante la realización del trabajo el autor recibió una beca académica del Consejo Nacional de Ciencia y Tecnología (181001) y del Instituto Potosino de Investigación Científica y Tecnológica, A. C.

IPICYT

Instituto Potosino de Investigación Científica y Tecnológica, A.C.

Acta de Examen de Grado

El Secretario Académico del Instituto Potosino de Investigación Científica y Tecnológica, A.C., certifica que en el Acta 050 del Libro Primero de Actas de Exámenes de Grado del Programa de Doctorado en Ciencias en Biología Molecular está asentado lo siguiente:

En la ciudad de San Luis Potosí a los 1 días del mes de febrero del año 2013, se reunió a las 16:15 horas en las instalaciones del Instituto Potosino de Investigación Científica y Tecnológica, A.C., el Jurado integrado por:

Dr. Samuel Lara González	**Presidente**	**IPICYT**
Dr. Marco Martín González Chávez	**Secretario**	**UASLP**
Dr. Carlos Barajas López	**Sinodal**	**IPICYT**
Dr. Roberto Martínez	**Sinodal externo**	**UNAM**

a fin de efectuar el examen, que para obtener el Grado de:

DOCTOR EN CIENCIAS EN BIOLOGÍA MOLECULAR

sustentó el C.

Juan Francisco Ramírez Martínez

sobre la Tesis intitulada:

Synthesis and Electrophysiological Evaluation of 6,11-Dihydrodibenzo[c,f][1,2,5]thiadiazepine-5,5-dioxide (DBTD): Non-Competitive GABAA Receptor Antagonists

que se desarrolló bajo la dirección de

Dr. Carlos Barajas López

El Jurado, después de deliberar, determinó

APROBARLO

Dándose por terminado el acto a las 18:20 horas, procediendo a la firma del Acta los integrantes del Jurado. Dando fe el Secretario Académico del Instituto.

A petición del interesado y para los fines que al mismo convengan, se extiende el presente documento en la ciudad de San Luis Potosí, S.L.P., México, a los 1 días del mes de febrero de 2013.

Dr. Marcial Bonilla Marín
Secretario Académico

INSTITUTO POTOSINO DE INVESTIGACIÓN CIENTÍFICA Y TECNOLÓGICA, A.C.
IPICYT
SECRETARIA ACADEMICA

Mtra. Ivonne Lizette Cuevas Vélez
Jefa del Departamento del Posgrado

Dedicatorias

A MIS PADRES DELFINA Y GIL

A MI ESPOSA COCO

A MIS HIJOS LEO Y SOPHIE

A MIS HERMANOS MIGUEL Y EDUARDO

A TODOS MIS FAMILIARES

A MIS COMPAÑEROS DE LABORATORIO

A MIS REALES Y DURADEROS AMIGOS

A TODOS MIS PROFESORES

A MI PATRIA Y A MI TERRUÑO SAN LUIS POTOSÍ

AL CREADOR DE TODA ESTA ENERGÍA

"LO ESENCIAL ES INVISIBLE PARA LOS OJOS"

ANTOINE DE SAINT-EXUPÉRY

Agradecimientos

Del Laboratorio de Neurobiología (DBM, IPICyT) a:

- ✓ Dr. Carlos Barajas López, por el apoyo y confianza recibidos al permitirme trabajar en su grupo de investigación y de esta forma aprender una parte referente al amplio mundo de la electrofisiología neuronal
- ✓ Rosa Espinosa Luna, por su ayuda incondicional y consejo a lo largo del proyecto
- ✓ Marcela, Esri y Raquel, por el apoyo que me brindaron en diferentes etapas del proyecto

Del Laboratorio de Síntesis Orgánica (CIEP, UASLP) a:

- ✓ Dr. Marco Martín González Chávez, por el apoyo incondicional que me ha brindado a lo largo de los años en todos los proyectos de investigación que he realizado
- ✓ L.Q. Rodolfo González Chávez, por su apoyo e incondicional ayuda en la parte sintética y de cálculos teóricos
- ✓ Estela Nuñez Pastrana y María Guadalupe Ortega Salazar por su apoyo experimental

Del Instituto de Química (UNAM) a:

- ✓ Dr. Roberto Martínez, Dr. Paul E. Reyes, A. Peña, E. Huerta, E. Hernández, L. Velasco, y J. Pérez por su apoyo en la obtención de espectros de RMN-^{1}H, RMN-^{13}C, E.M. y análisis elemental.

A CONACYT por la beca otorgada (181001) y por apoyo con el proyecto no. 134687

A la UASLP por el apoyo vía FAI (C03-FAI-11-21.56) y PIFI 2.0

Content

List of figures, schemes, and tables

Abbreviations

Abbreviation	Meaning
$[D_6]$DMSO	Deuterated Dimethyl sulfoxide
^{13}C NMR	Carbon 13 Nuclear Magnetic Resonance Spectroscopy
^{1}H NMR	Proton Nuclear Magnetic Resonance Spectroscopy
ATP	adenosine-5'-triphosphate
$CDCl_3$	Deuterated chloroform
DBTDs or 2	dibenzo[c,f][1,2,5]thiadiazepines
EC_{50}	half maximal effective concentration
EGTA	ethylene glycol-bis(2-aminoethylether)-N,N,N',N'-tetra-acetic acid
EPSP	excitatory postsynaptic potentials
eV	Electron volt
FTIR	Fourier Transform Infrared Spectroscopy
GABA	γ-aminobutíric acid
GABARAP	$GABA_A$ receptor associated protein
GTP	guanosine-5'-triphosphate
HEPES	hydroxyethyl piperazineethanesulfonic acid
IC_{50}	half maximal inhibitory concentration
I_{GABA}	currents induced by GABA
IPSP	Inhibitory postsynaptic potentials
MS	mass spectra
PKC	Protein kinase C
SEM	standard error of the mean

Resumen

Synthesis and Electrophysiological Evaluation of 6,11-Dihydrodibenzo[c,f][1,2,5]thiadiazepine-5,5-dioxide (DBTD): Non-Competitive $GABA_A$ Receptor Antagonists

En este trabajo describimos un nuevo proceso para obtener dibenzo[c,f][1,2,5]tiadiazepinas (DBTDs o **2**) y sus efectos como modulador de los receptores $GABA_A$ de neuronas mientéricas de cobayo. La síntesis de derivados de DBTDs inició con dos compuestos aromáticos comerciales. Un grupo azida fue obtenido después de dos reacciones secuenciales y posteriormente el anillo central fue cerrado vía nitrenos obteniendo sulfonamidas tricíclicas (DBTDs). Los resultados de experimentos de célula completa en neuronas mostraron que la aplicación de **2** no afecta la corriente neuronal basal pero inhiben las corrientes inducidas por GABA (I_{GABA}), las cuales son mediadas por receptores $GABA_A$. Los efectos de las DBTDs alcanzaron su máximo a los 3 min después de su aplicación y fueron: i) reversibles; ii) dependiente de la concentración (con un orden de potencia de **2c** = **2d** > **2b**); iii) antagonismo no competitivo y; iv) solo se presenta cuando **2** fue aplicado extracelularmente. Picrotoxina y **2** no afectan sus efectos inhibitorios cuando ambos se aplican. Nuestros resultados indican que DBTD actúa en la región extracelular de los canales GABA distinto al poro, pero independiente del sitio de unión de la picrotoxina, benzodiazepina y sitios de unión a GABA. Las DBTDs descritas aquí pudieran ser empleadas como un modelo inicial para sintetizar nuevos inhibidores de los receptores $GABA_A$ con potencial para ser usados como antídotos en la intoxicación por moduladores positivos de estos receptores o inducir epilepsia experimental.

PALABRAS CLAVE.

Dibenzotiadiazepinas, Receptores $GABA_A$, Neuroquímica, Actividad Biológica, Neuronas entéricas, Patch clamp, Antagonistas de los receptores $GABA_A$, Electrofisiología.

Abstract

Synthesis and Electrophysiological Evaluation of 6,11-Dihydrodibenzo[c,f][1,2,5]thiadiazepine-5,5-dioxide (DBTD): Non-Competitive $GABA_A$ Receptor Antagonists

A new process for obtaining dibenzo[c,f][1,2,5]thiadiazepines (DBTDs or **2**) and their effects as modulators on $GABA_A$ receptors of guinea pig myenteric neurons are described. Synthesis of DBTD derivatives began with two commercial aromatic compounds. An azide group was obtained after two sequential reactions, and the central ring was closed via nitrene to obtain the tricyclic sulfonamides (DBTDs). Whole-cell neuronal recordings showed that **2** application did not affect the holding neuronal current but inhibited the currents induced by GABA (I_{GABA}), which are mediated by $GABA_A$ receptors. These DBTDs effects reached their maximum 3 min after application and were: i) reversible, ii) concentration-dependent (with a rank order of potency of **2c** = **2d** > **2b**), iii) mediated by a non-competitive antagonism, and iv) only observed when applied extracellularly. Picrotoxin (which binds in the channel mouth) and DBTDs effects were not modified when both substances were simultaneous applied. Our results indicate that DBTD acted on the extracellular domain of $GABA_A$ channels but independent of the picrotoxin, benzodiazepine, and GABA binding sites. DBTDs used here could be the initial model for synthesizing new $GABA_A$ receptor inhibitors with a potential to be used as antidotes for positive modulators of these receptors or to induce experimental epilepsy.

Keywords

Dibenzothiadiazepines, $GABA_A$ receptors, neurochemistry, Biological activity, Enteric neurons, Patch clamp, $GABA_A$ receptor antagonists, Electrophysiology.

CHAPTER 1 BACKGROUND

1.1 Ligand Gated Channels are Essential for Neuronal Communication

Fast synaptic transmission is mediated by neurotransmitters, which activate ionic channels in the postsynaptic membrane. The opening of these Ligand Gated Channels (LGC) modifies the membrane potential of the postsynaptic cell, which results in excitatory or inhibitory postsynaptic potentials (EPSP and IPSP, respectively). There are different LGC in the neuronal tissue: i) the superfamily of the *Cys-loop* (p.e. nicotínicos), ii) those activated by nucleotides named purinergic (P2X), and iii) those activated by glutamate, cknown as glutamatergic. The properties of *Cys-loop* receptors, in particular those of $GABA_A$ receptors, activaed by γ-aminobutíric acid (GABA) will be revised here.

Cys-loop receptors are composed of five subunits that share several structural properties. Each subunit possesses certain structural properties that are well conserved for all members of this family. For instance, subunits are all composed of an extracellular amino terminus, four transmembranous domains (M1-M4), and an extracellular carboxyl terminus (Le Novere et al., 2002; Ortells and Lunt, 1995). Between transmembrane domains, M3 and M4 there is a long intracellular loop that allows for interaction with the proteins of the intracellular matrix. There are some important functional differences among *Cys-loop* receptors. Thus, some are permeable to cations (p.e. nACh receptors) and mediate EPSPs, and others (p.e. $GABA_A$ receptors) are permeable to cloride and mediate IPSPs

(Karanjia et al., 2006; Le Novere et al., 2002; Miranda-Morales et al., 2007; Ortells and Lunt, 1995).

Thus far, there are twenty known $GABA_A$ subunits grouped into seven families based on their structural similarities (α1-6, β1-4, γ1-3, ρ1-3, ε, π, θ, δ). Each one of these subunits shows a particular localization to specific areas in the nervous system. The ρ subunit, for instance, was initially only found in the retina, are functionally distinct to other $GABA_A$ receptors, and was known as $GABA_C$ previously (Hanley et al., 1999). The most common native receptor stoichiometry is two α, two β and one of either γ, δ, or ε (Farrar et al., 1999).

Different stoichiometry of $GABA_A$ receptors provides different pharmacological and functional properties, affecting the overall efficacy and affinity of agonists and antagonists, and the channels properties (Enna, 2012). Thus, α subunits have been shown to impart different receptor efficacies for partial agonists like (RS)-dihydromuscimol, piperidine-4-sulfonic acid and 4,5,6,7-tetrahydroisoxazolo [5,4-c] pyridin-3-ol (Ebert et al., 1994). Changing the β subunit has also been reported to affect the potency for GABA and the maximum current obtained (Ducic et al., 1995; Hadingham et al., 1993; Jensen et al., 2002). The β subunit has also been shown to impart the ion selectivity of the $GABA_A$ channel (Jensen et al., 2002). Likewise, the presence of the γ subunit, specifically γ2, appears to be important for benzodiazepine potentiation of the GABA response (Kofuji et al., 1991; Sigel et al., 1990). Collectively, the characteristics of the GABA channels are dependent on the subunits present.

Additional subunit diversity can be obtained by splicing variations. The γ_2 subunit exist in two forms, a short γ_{2S} and a long γ_{2L} form (Kofuji et al., 1991; Sigel et al., 1990). The addition of a twenty-four base-pair (eight amino acid) exon provides the γ_{2L} isoform with a new regulatory region, a calcium dependent PKC phosphorylation site in the large cytoplasmic loop (Swope et al., 1999).

The localization of the $GABA_A$ receptors in the postsynaptic membrane appears to be dependent on the presence of a tubulin binding protein called gephyrin (Kneussel et al., 1999). This protein was originally identified as being required for the localization of the glycine channels (Kirsch et al., 1991) and latter, it was shown to be required for the clustering of $GABA_A$ channels at GABAergic synapses (Kneussel et al., 1999). It is postulated that the interaction of $GABA_A$ channels is dependent on the association of the γ subunit with a protein called $GABA_A$ receptor associated protein (GABARAP) (Wang et al., 1999). GABARAP has protein homology with microtubule-associated proteins (MAPs) and has been postulated that GABARAP functions as a protein-cytoskeleton linker. This is a similar function to what MAP1-B, which has been shown, to be associated with the anchoring of $GABA_C$ receptors (Hanley et al., 1999). At present, it is unclear whether the tubulin binding functions of gephyrin, GABARAP, MAP1-B and possibly other MAPs are essential for $GABA_A$ subunit anchoring. In either case there is strong evidence implicating gephyrin in the clustering of $GABA_A$ receptors (Kneussel et al., 1999).

1.2 Pharmacological Importance of $GABA_A$ Receptors

$GABA_A$ are expressed in both central and peripheral nervous systems. These receptors mediate most of the effects of GABA in the brain. Its pharmacological importance is well recognized because they are the targets for therapeutic effects of benzodiazepines, phenobarbital, and various general anesthetics. In addition, $GABA_A$ receptors have been implicated in numerous pathological processes such as: epilepsia, han sido implicados en numerosos procesos patológicos tales como la epilepsy, anxiety, major depression, pain, and as target of psychotropic substances (Enna, 2012; Krivoshein and Hess, 2006; Mohler, 2011; Twyman et al., 1989). The role of $GABA_A$ channels in the peripheral nervous system is unknown (Sokolova et al., 2001). However, their expression in primary sensory neurons suggests that they might be used as targets to control the sensory activity by synthetic substances.

1.3 Enteric Neurons

Synaptic communication in enteric neurons is not a simple matter, with some studies suggesting that the number of neurons and associated glia in the system rivals that of the spinal cord (Galligan, 2002). All three types of synaptic communication are present in the enteric nervous system and employ various channels and neurotransmitters (Galligan, 2002; Shen and Surprenant, 1993). The majority of the synapses in the enteric nervous system are located in two ganglionated plexuses, the myenteric and submucosal. These plexus play distinct set of functions; namely, the myenteric plexus appears to be responsible for the control of gastrointestinal motility while the other mediates the gastrointestinal

epithelium functions, neuroimmune responses and local blood flow (Cooke, 1998; Galligan, 2002).

There are two major classes of enteric neurons; S neurons and AH neurons (Nishi and North, 1973). Extensive characterizations of both S and AH neurons have been published (Brookes, 2001; Costa et al., 1996; Furness et al., 1998). Functionally, S type neurons appear to function as interneurons and motor neurons, and AH type neurons function as intrinsic sensory neurons (Brookes, 2001; Costa et al., 1996; Furness et al., 1998).

1.3.1 Enteric $GABA_A$ receptors

The function of GABA in the enteric nervous system is unclear. $GABA_A$ channels have been shown to be present mainly in AH neurons in the myenteric plexus but are found on both S and AH neurons in the submucosal plexus (Cherubini and North, 1984).

Through the use of reverse transcriptase polymerase chain reaction (RT-PCR) and *in-situ* hybridization it has been shown that α1, α3, α5, β2 and γ3 are expressed in both myenteric and submucosal plexuses. In addition the β3 and γ1 subunits have been found in the myenteric but not submucosal plexus (Poulter et al., 1999). Furthermore, a number of putative intrinsic primary afferents and nitric oxide synthase (NOS) immunoreactive inhibitory motor neurons have been shown to express ρ subunits (Fletcher et al., 2001). Up to date, pharmacological studies have not identified the functional role of the ρ subunits in the gut.

The exogenous application of GABA is able to elicit a chloride mediated current and GABA has been found to mediate contraction in *ex-vivo* longitudinal muscle preparations (Karanjia et al., 2006; Miranda-Morales et al., 2007; Tsai et al., 1993; Zhou and Galligan, 2000). These effects have been pharmacologically identified as being mediated by either $GABA_A$ or $GABA_B$. $GABA_A$ mediated synaptic responses have not been found in the enteric nervous system (Galligan, 2002), yet the large number of $GABA_A$ channels suggests some role for GABA in the gut. Indeed GABA has been implicated as a mediator of intestinal motility and has been shown to affect the secretion of acetylcholine gastrin and somatostatin from the gut (Harty et al., 1991; Harty and Franklin, 1983; Poulter et al., 1999). Here, we used enteric $GABA_A$ channels as a model to investigate the effect of DBTDs on sensory primary neurons.

1.4 Biological relevance of dibenzothiadiazepines

Tricyclic compounds with a central thiadiazepine ring (Figure 1, **1** ring B) were first described in Weber's 1966 publication of the synthesis of dibenzothiadiazepines (DBTDs) (Weber, 1966a), followed by a description of the compounds anti-depressive effects (**1a**) (Weber, 1966b; Weber and Frossard, 1966).

In 1991, Giannotti et al. (Giannotti et al., 1991) prepared DBTD (**1b**) structural variants at nitrogen 11 (N-11) with the purpose of increasing the antidepressive effects previously observed by Weber while reducing possible side effects. In addition to the effects of DBTDs on the central nervous system, these substances were found to act as non-nucleosidic reverse transcriptase inhibitors of HIV-1 (**1c**) (Bellarosa et al., 1996) and to have anti-proliferative activity on

leukemia cell lines (**1d**) (Silvestri et al., 2006). Effects that increased the attention toward these tricyclic compounds.

The central ring of DBTDs has been synthesized via the Goldberg method (Goldberg, 1906), which involves an Ullmann intra-molecular condensation reaction (N-C) (Figure 2, via a) (Goldberg, 1906). This reaction is limited by the fact that ortho-haloanilines significantly reduce number of possible substituents that may be included in the DBTDs. Only one report has described the use of this methodology for obtaining compounds **2a** and **2d** (Altamura et al., 2009). As an alternative approach, N-C bonds may be formed via intra-molecular reactions of aryl azides with benzene derivatives (Figure 2, via b), which has been described during the formation of carbazoles through thermolysis (Jian and Tour, 2003), photolysis (Tsao et al., 2003), and recently, via metal catalysis (Shou et al., 2009; Stokes et al., 2009). The advantage of using aryl azides is that C-N bonds form directly. Therefore, the use of monosubstituted anilines with diverse functional groups can lead us toward obtaining DBTDs with functional variations in the C ring. Known DBTDs and triheterocyclic analogous compounds include diverse substituents on the nitrogen of the thiadiazepine ring (Figure 1); however, no studies have examined the biological activities of the parent compound and 9-substituted derivatives (Figure 2). This work is the first report to consider a biological study of DBTDs without substituents on nitrogens 6 and 11 of B ring, which were obtained through a distinct process than the Ullmann method. The presence of a hydrogen atom at N-6 and N-11 in a DBTD can determine the

compound's affinity toward proteins via hydrogen bond interactions (Cherney et al., 2003), as shown in Figure 3.

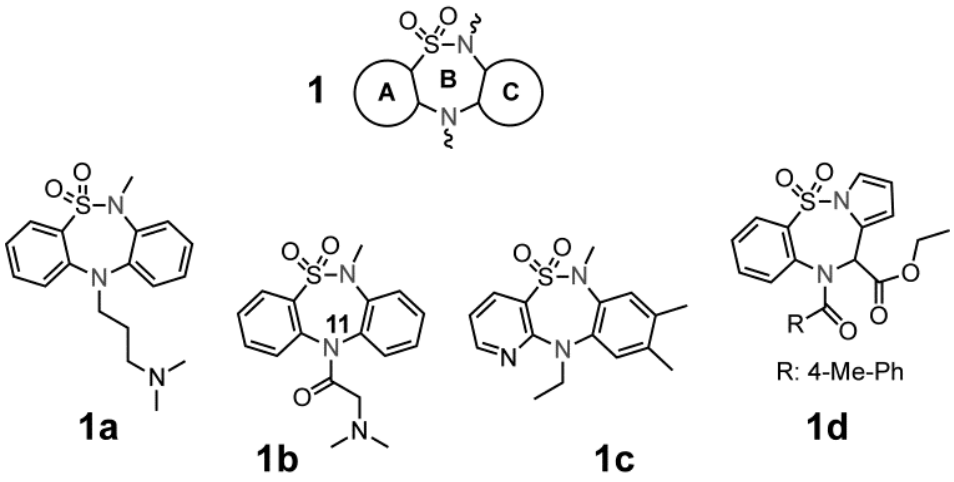

Figure 1. General chemical structure of the dibenzo[*c,f*][1,2,5]thiadiazepines **1**, and several DBTDs reported to have biological activity (**1a**, **1b**, **1c**, and **1d**).

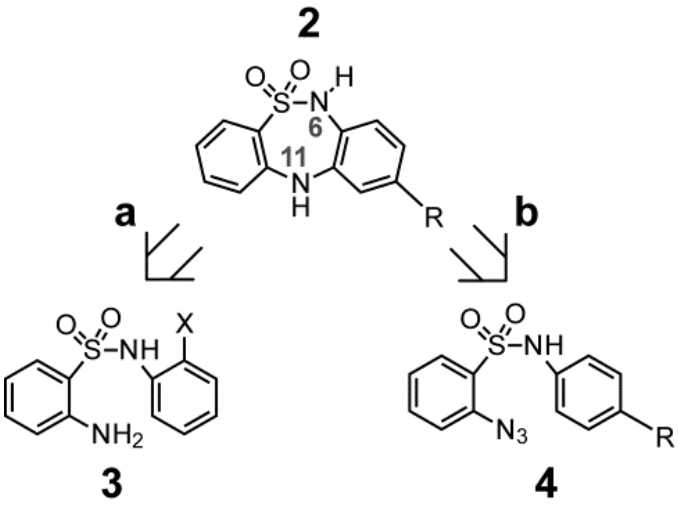

Figure 2. Retrosynthetic analysis of the non-substituted DBTDs. a) Classical method for obtaining **2** by the Goldberg methodology; b) Obtaining **2** from an aryl azide.

The linear synthetic route to the DBTDs **2a–2g** comprises four stages and proceeds as described in Scheme 1. The thiadiazepine ring is formed through direct amination of the C ring via intramolecular thermal cyclization of **4** (Figure 2, via b). This methodology provides an alternative to the classical amination of Goldberg approach, with respect the formation of ring B in the substituted DBTDs (Figure 2, via **a**) (Altamura et al., 2009; Bellarosa et al., 1996; Giannotti et al., 1995; Giannotti et al., 1991; Weber and Frossard, 1966).

DBTDs with a modified B ring were shown to have biological effects. Giannotti et al. synthesized a series of DBTDs with substituents in the thiadiazepine ring, and they showed that the compounds displayed a potential antidepressive effect using the apomorphine-induced hypothermia test (Giannotti et al., 1991). However, these authors found no binding of DBTDs with receptors to dopamine, serotonin, histamine, benzodiazepine, GABA, acetylcholine, and adrenaline, and reported that DBTDs lack effect on serotonin and noradrenaline uptake. However, such observations does not rule out that DBTDs might be modulating any of these receptor proteins through a different binding site than the one directly-activated by a given agonist or modulator.

At least three observations indicated us that $GABA_A$ channels might be the target for DBTDs: i) the tricyclic sulfonamide **2** is structurally similar to the 1,4-benzodiazepines, which are major positive modulators of these channels (Enna, 2012); ii) DBTDs have antidepressive actions (Giannotti et al., 1991), and $GABA_A$

channels have been implicated in mood disorders, including depression (Brickley and Mody, 2012; Krystal et al., 2002). Therefore, the aim of the present study was to further investigate the effects of DBTDs on $GABA_A$ channels and to report a new synthetic platform for obtaining DBTD compounds that do not include the thiadiazepine ring substitutions. We found that these compounds inhibit directly $GABA_A$ channels by a mechanism that is independent of the binding sites for GABA, picrotoxin, and benzodiazepine.

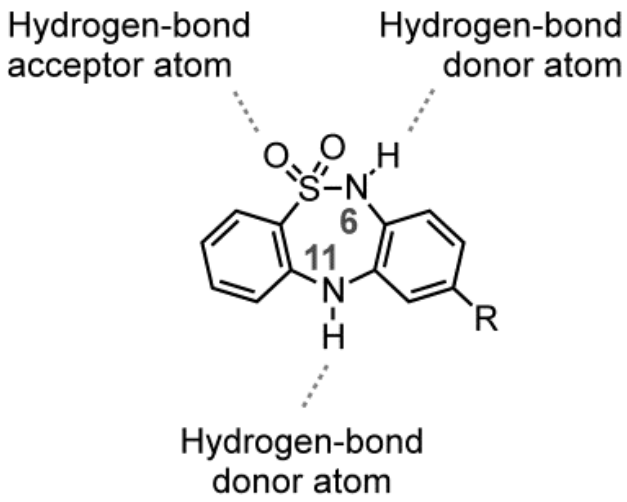

Figure 3. The dotted lines in **2** indicate probable interactions between hydrogen bonds and proteins.

RATIONALE

A series of DBTDs with substituents in the thiadiazepine ring displayed a potential antidepressive. However, there is not binding of these compounds with receptors to dopamine, serotonin, histamine, benzodiazepine, GABA, acetylcholine, and adrenaline, and do not have any effect on serotonin and noradrenaline uptake. This lack of binding does not rule out that DBTDs might be modulating any of these receptor proteins through a different binding site than the one activated by a given agonist or modulator. For instance, $GABA_A$ channels have various binding sites that could be the target for DBTDs.

HYPOTHESIS

Since DBTDs does not bind to GABA receptors DBTDs regulate $GABA_A$ channels by binding to modulatory site.

OBJECTIVES

1) To report a new synthetic platform for obtaining DBTD compounds that do not include the thiadiazepine ring substitutions.

2) To investigate the effects and possible mechanism of action of DBTDs on enteric $GABA_A$ channels.

CHAPTER 2 MATERIAL AND METHODS

2.1 Chemical Methods

2.1.1 General Procedures

All reagents and solvents were reagent-grade and were used as received from Sigma-Aldrich Co. (St. Louis, MO, USA). Flash chromatography was performed using Merk Kiesegel 60 silica gel (230–400 mesh). Melting points are reported uncorrected. The FTIR spectra were recorded on a Thermo Nicolet Nexus 470 FTIR as thin films on a KBr disk (for solids) or a germanium ATR crystal (for liquids). ^{1}H NMR and ^{13}C NMR spectra were obtained using an Eclipse Jeol (operating at 300 and 75 MHz, respectively) and a Varian-Gemini (operated at 200 MHz and 50 MHz, respectively), and the signals are reported in ppm relative to TMS. All mass spectra (MS) were recorded on a Jeol AX505HA mass spectrometer. Elemental analyses were performed on a CE-440 Exeter Analytical Inc.

2.1.2 General Procedures for Synthesizing N-(4-(R)phenyl)-2-nitrobenzenesulfonamides (5a–5f)

Anhydrous pyridine (1.10 mL, 13.6 mmol) and 4-R-aniline (1.24 mL, 13.6 mmol) in dry acetone were added, via cannula, to a stirred solution of 2-nitrobenzenesulfonyl chloride (3.01 g, 13.6 mmol) in dry acetone under nitrogen, and the reaction mixture was stirred at room temperature. After 24 h the mixture was neutralized with a saturated sodium bicarbonate solution, and the resulting solid was collected,

washed with water and ethanol, and dried under vacuum. The solid was purified by flash chromatography (silica gel, eluting with 90:10 hexane–ethyl acetate), then recrystallized from ethyl acetate–hexane (30:70) to obtain **5a** as a white solid (11.97 mmol, 88%); mp: 118–119 °C. The same procedure was used for the synthesis of **5b–5f**.

Products **5**, **6**, and **4** (except for series **f)** were first reported by Saeed and N.H. Rama (Saeed and Rama, 1997). However, **5** and **6** not were characterized and compound **4** was only partially characterized by IR and MS spectroscopies.

***N*-(phenyl)-2-nitrobenzenesulfonamide (5a):** ^{1}H NMR (300 MHz, $CDCl_3$+[D_6]DMSO): *d* = 7.08 (m, 1H), 7.21 (m, 4H), 7.63 (ddd, J_o= 7.5 Hz, J_m= 1.6 Hz, 1H), 7.70 (ddd, J_o= 7.5 Hz, J_m= 1.6 Hz, 1H), 7.76 (dd, J_o= 8.0 Hz, J_m= 1.6 Hz, 1H), 7.92 (dd, J_o= 7.9 Hz, J_m= 1.6 Hz, 1H), 9.9 ppm (s, 1H); IR (KBr): ν = 3324, 1380, 1180 cm^{-1}; MS (EI, 70 eV): *m/z*: 278 [M]$^+$.

***N*-(4-fluorophenyl)-2-nitrobenzenesulfonamide (5b):** Yellow crystals. Yield 79%; mp: 106 ºC; ^{1}H NMR (200 MHz, [D_6]DMSO): *d* = 7.13 (d, J_o= 6.8 Hz, 4H), 7.88 (m, 4H), 10.7 ppm (s, 1H); IR (KBr): ν = 3293, 1360, 1160 cm^{-1}; MS (EI, 70 eV): *m/z*: 296 [M]$^+$.

***N*-(4-chlorophenyl)-2-nitrobenzenesulfonamide (5c):** Yellow crystals. Yield 66%; mp: 122 ºC; ^{1}H NMR (200 MHz, [D_6]DMSO): *d* = 7.13 (d, J_o= 9.0 Hz, 2H), 7.35 (d, J_o= 9.0 Hz, 2H), 7.89 (m, 4H), 10.9 ppm (s, 1H); IR (KBr): ν = 3309, 1334, 1162 cm^{-1}; MS (EI, 70 eV): *m/z*: 312 [M]$^+$.

***N*-(4-bromophenyl)-2-nitrobenzenesulfonamide (5d):** Colorless crystals. Yield 79%; mp: 118 ºC; ^{1}H NMR (200 MHz, [D_6] DMSO): *d* = 7.06 (d, J_o= 9.0 Hz, 2H), 7.47 (d, J_o= 8.8 Hz, 2H), 7.91 (m, 4H), 10.9 ppm (s, 1H); IR (KBr): ν = 3297, 1363, 1164 cm^{-1}. MS (EI, 70 eV): *m/z*: 358/356 [M]$^+$.

***N*-(4-methoxyphenyl)-2-nitrobenzenesulfonamide (5e):** Yellow needle crystals. Yield 72%; mp: 90 ºC; ^{1}H NMR (200 MHz, [D_6]DMSO): *d* = 3.67 (s, 3H), 6.83 (d, J_o= 9.0 Hz, 2H), 7.03 (d, J_o= 9.0 Hz, 2H), 7.87 (m, 4H), 10.4 ppm (s, 1H); IR (KBr): ν = 3259, 1361, 1172 cm^{-1}; MS (EI, 70 eV): *m/z*: 308 [M]$^+$.

Ethyl-4-(2-nitrophenylsulfonamido)benzoate *N* (5f): brown solid. Yield 82%; mp: 172 ºC; ^{1}H NMR (300 MHz, [D_6]DMSO): *d* = 1.25 (t, J_o= 7.1 Hz, 3H), 4.22 (q, J_o= 7.1 Hz, 2H), 7.13 (BB', J_o= 8.7 Hz, 2H), 7.75 (ddd, J_o= 7.5 Hz, 1H), 7.78 (AA', J_o= 8.7 Hz, 2H), 7.79 (ddd, J_o= 7.5 Hz, 1H), 7.91 (dd, J_o= 6.6 Hz, 1H), 7.98 ppm (dd, J_o= 7.0 Hz, 1H); IR (KBr): ν = 3200, 1690, 1365, 1162 cm^{-1}; MS (EI, 70 eV): *m/z*: 350 [M]$^+$.

2.1.3 General Procedures for the Synthesis of 2-amino-N-(4-(R) phenyl)benzenesulfonamide (6a–6f)

N-(4-(R) phenyl)-2-nitrobenzenesulfonamide **5** (4.3 g, 15.6 mmol) and tin (II) chloride dehydrate (14.82 g, 65.7 mmol) were heated in ethyl acetate under reflux for 4 h. The mixture was stirred, and a saturated sodium bicarbonate solution was added to a pH of 6. The solution was extracted with ethyl acetate. The solvent was removed, and the residue was purified by flash chromatography (eluting with a 90:10 solution of hexane–ethyl acetate).

2-amino-*N*-phenylbenzenesulfonamide (6a): Yellow powder (14.04 mmol, 90%); mp: 123-124 ºC; ^{1}H NMR (300 MHz, [D$_6$]DMSO): *d* = 5.99 (s, 2H), 6.54 (ddd, J_o= 7.6 Hz, J_m= 1.2 Hz, 1H), 6.75 (dd, J_o= 8.1 Hz, J_m= 0.9 Hz, 1H), 6.97 (ddd, J_o= 8.2 Hz, 1H), 7.04 (dd, J_o= 8.6 Hz, 2H), 7.2 (m, 3H), 7.49 (dd, J_o= 8.5 Hz, J_m= 1.4 Hz, 1H), 10.2 ppm (s, 1H); IR (KBr): ν = 3457, 3368, 3240, 1360, 1180 cm^{-1}; MS (EI, 70 eV): *m/z*: 248 [M]$^+$.

2-amino-*N*-(4-fluorophenyl) benzenesulfonamide (6b): Brown liquid. Yield 99%; ^{1}H NMR (200 MHz, [D$_6$]DMSO): *d* = 5.98 (s, 2H), 6.53 (ddd, J_o= 7.05 Hz, J_m= 1.2 Hz, 1H), 6.74 (dd, J_o= 8.3 Hz, J_m= 1.2 Hz, 1H), 7.05 (d, J_o= 6.4 Hz, 4H), 7.21 (ddd, J_o= 7.0 Hz, J_m= 1.6 Hz, 1H), 7.43 (dd, J_o= 8.2 Hz, J_m= 1.6 Hz, 1H), 10.2 ppm (s, 1H); IR (KBr): ν = 3469, 3382, 3284, 1313, 1147 cm^{-1}; MS (EI, 70 eV): *m/z*: 266 [M]$^+$.

2-amino-*N*-(4-chlorophenyl) benzenesulfonamide (6c): Brown liquid. Yield 99%; ^{1}H NMR (200 MHz, [D$_6$]DMSO): *d* = 6.0 (s, 2H), 6.53 (ddd, J_o= 8.0 Hz, J_m= 1.1, 1H), 6.73 (dd, J_o= 8.3 Hz, J_m= 0.9 Hz, 1H), 7.03 (d, J_o= 8.8 Hz, 2H), 7.2 (ddd, J_o= 8.5 Hz, J_m= 1.6, 1H), 7.26 (d, J_o= 8.8 Hz, 2H), 7.47 (dd, J_o= 8.0 Hz, J_m= 1.6, 1H), 10.4 ppm (s, 1H); IR (KBr): ν = 3467, 3378, 3245, 1313, 1135 cm^{-1}; MS (EI, 70 eV): *m/z*: 282 [M]$^+$.

2-amino-*N*-(4-bromophenyl) benzenesulfonamide (6d): Brown liquid. Yield 99%; ^{1}H NMR (200 MHz, [D$_6$]DMSO): *d* = 6.0 (s, 2H), 6.55 (ddd, J_o= 7.8 Hz, 1H), 6.76 (dd, J_o= 8.3 Hz, J_m= 0.9 Hz, 1H), 7.0 (d, J_o= 8.8 Hz, 2H), 7.21 (ddd, J_o= 7.0 Hz, J_m= 1.6 Hz, 1H), 7.39 (d, J_o= 8.8 Hz, 2H), 7.49 (dd, J_o= 7.9 Hz, J_m= 1.5 Hz, 1H), 10.4

ppm (s, 1H); IR (KBr): ν = 3482, 3384, 3268, 1319, 1139 cm^{-1}; MS (EI, 70 eV): *m/z*: 328/326 $[M]^+$.

2-amino-*N*-(4-methoxyphenyl) benzenesulfonamide (6e): Brown liquid. Yield 99%; ^1H NMR (200 MHz, $[D_6]$DMSO): *d* = 3.65 (s, 3H), 5.9 (s, 2H), 6.5 (ddd, J_o= 7.7 Hz, J_m= 1.2 Hz, 1H), 6.72 (dd, J_o= 8.7 Hz, 1H), 6.77 (d, J_o= 9.0 Hz, 2H), 6.95 (d, J_o= 9.0 Hz, 2H), 7.19 (ddd, J_o= 8.2 Hz, J_m= 1.6 Hz, 1H), 7.36 (dd, J_o= 8.1 Hz, J_m= 1.6 Hz, 1H), 9.84 ppm (s, 1H); IR (KBr): ν = 3480, 3380, 3266, 1321, 1147 cm^{-1}; MS (EI, 70 eV): *m/z*: 278 $[M]^+$.

Ethyl-4-(2-aminophenylsulfonamido)benzoate (6f): Yellow crystals. Yield 88%; mp: 163 °C; ^1H NMR (200 MHz, $[D_6]$DMSO): *d* = 1.25 (t, J_o= 6.3 Hz, 3H), 4.22 (q, J_o= 7.0 Hz, 2H), 6.0 (s, 2H), 6.56 (ddd, J_o= 7.6 Hz, 1H), 6.73 (dd, J_o= 7.8 Hz, 1H), 7.14 (BB', J_o= 8.8 Hz, 2H), 7.22 (ddd, J_o= 7.7 Hz, 1H), 7.57 (dd, J_o= 8.1 Hz, J_m= 1.6 Hz, 1H), 7.79 (AA', J_o= 8.8 Hz, 2H), 10.8 ppm (s, 1H); IR (KBr): ν = 3470, 3380, 3230, 1690, 1322, 1144 cm^{-1}; MS (EI, 70 eV): *m/z*: 320 $[M]^+$.

2.1.4 General Procedures for Synthesizing 2-azido-N-(4-(R)phenyl)benzenesulfonamide (4a–4f)

An aqueous solution of sodium nitrite (3.6 g, 51.8 mmol) was added to 2-amino-*N*-(4-(R)phenyl)benzenesulfonamide **6** (2.86 g, 11.5 mmol) in trifluoroacetic acid, and the reaction mixture was stirred for 1 h. Sodium azide (1.9 g, 28.8 mmol) was added, and the solution was stirred for an additional 1 h. The mixture was neutralized with saturated sodium bicarbonate solution and extracted with ethyl acetate. The reaction mixture was concentrated and purified by flash

chromatography (70:30, hexane–ethyl acetate). The obtained solid was recrystallized in ethyl acetate–hexane (30:70).

2-azido-*N*-phenylbenzenesulfonamide (4a): Brown powder (9.78 mmol, 85%); mp: 139 ºC; ^{1}H NMR (200 MHz, [D$_6$]DMSO): *d* = 6.97 (ddd, J_o= 7.0 Hz, 1H), 7.1 (dd, J_o= 7.4 Hz, 2H), 7.2 (ddd, J_o= 7.4 Hz, 2H), 7.28 (ddd, J_o= 7.6 Hz, 1H), 7.5 (dd, J_o= 8.1 Hz, 1H), 7.64 (ddd, J_o= 7.8 Hz, 1H), 7.86 (dd, J_o= 7.8 Hz, 1H), 10.4 ppm (s, 1H); IR (KBr): ν = 3253, 2133, 1340, 1190 cm^{-1}; MS (EI, 70 eV): *m/z*: 274 [M]$^+$.

2-azido-*N*-(4-fluorophenyl) benzenesulfonamide (4b): White solid. Yield 83%; mp: 129 ºC; ^{1}H NMR (200 MHz, [D$_6$]DMSO): *d* = 7.09 (m, 4H), 7.27 (ddd, J_o= 7.3 Hz, J_m= 1.4 Hz, 1H), 7.52 (dd, J_o= 8.0 Hz, J_m= 1.0 Hz, 1H), 7.62 (ddd, J_o= 8.4 Hz, J_m= 1.6 Hz, 1H), 7.8 (dd, J_o= 7.8 Hz, J_m= 1.6 Hz, 1H), 10.2 ppm (s, 1H); IR (KBr): ν = 3249, 2140, 1334, 1166 cm^{-1}; MS (EI, 70 eV): *m/z*: 292 [M]$^+$.

2-azido-*N*-(4-chlorophenyl) benzenesulfonamide (4c): White crystals. Yield 80%; mp: 134 ºC; ^{1}H NMR (200 MHz, [D$_6$]DMSO): *d* = 7.11 (d, *Jo*= 8.8 Hz, 2H), 7.27 (d, J_o= 8.8 Hz, 2H), 7.31 (ddd, J_m= 1.1 Hz, 1H), 7.51 (dd, J_o= 8.0 Hz, J_m= 1.4 Hz, 1H), 7.66 (ddd, J_o= 7.7 Hz, J_m= 1.6 Hz, 1H), 7.86 (dd, J_o= 7.8 Hz, J_m= 1.4 Hz, 1H), 10.5 ppm (s, 1H); IR (KBr): ν = 3345, 2132, 1338, 1164 cm^{-1}; MS (EI, 70 eV): *m/z*: 308 [M]$^+$.

2-azido-*N*-(4-bromophenyl) benzenesulfonamide (4d): Yellow powder. Yield 87%; mp: 124 ºC; ^{1}H NMR (200 MHz, [D$_6$]DMSO): *d* = 7.05 (d, J_o= 8.8 Hz, 2H), 7.29 (ddd, J_o= 7.0 Hz, J_m= 1.2 Hz, 1H), 7.4 (d, J_o= 8.8 Hz, 2H), 7.52 (dd, J_o= 8.0 Hz, J_m= 1.2 Hz, 1H), 7.67 (ddd, J_o= 6.8 Hz, J_m= 1.4 Hz, 1H), 7.86 (dd, J_o= 7.8 Hz,

J_m= 1.6 Hz, 1H), 10.5 ppm (s, 1H); IR (KBr): ν = 3338, 2132, 1338, 1164 cm^{-1}; MS (EI, 70 eV): *m/z*: 354/352 $[M]^+$.

2-azido-*N*-(4-methoxyphenyl) benzenesulfonamide (4e): Brown crystals. Yield 78%; mp: 130 °C; ^{1}H NMR (200 MHz, $[D_6]$DMSO): *d* = 3.63 (s, 3H), 6.76 (d, J_o= 9.3 Hz, 2H), 7.01 (d, J_o= 8.7 Hz, 2H), 7.23 (ddd, J_o= 7.4, J_m= 1.1 Hz, 1H), 7.51 (dd, J_o= 7.9 Hz, J_m= 1.1 Hz, 1H), 7.62 (ddd, J_o= 7.8 Hz, J_m= 1.6 Hz, 1H), 7.73 (dd, J_o= 7.9 Hz, J_m= 1.2 Hz, 1H), 9.87 ppm (s, 1H); IR (KBr): ν = 3274, 2138, 1336, 1164 cm^{-1}; MS (EI, 70 eV): *m/z*: 304 $[M]^+$.

Ethyl-4-(2-azidophenylsulfonamido) benzoate (4f): Brown crystals. Yield 78%; mp: 182-184 ºC; ^{1}H NMR (200 MHz, $[D_6]$DMSO): *d* = 1.23 (t, J_o= 7.0 Hz, 3H), 4.20 (q, J_o= 7.1 Hz, 2H), 7.19 (BB', J_o= 8.7 Hz, 2H), 7.30 (ddd, J_o= 7.8 Hz, 1H), 7.48 (dd, J_o= 8.1 Hz, 1H), 7.65 (ddd, J_o= 7.8 Hz, 1H), 7.77 (AA', J_o= 8.7 Hz, 2H), 7.94 (dd, J_o= 7.8 Hz, 1H), 10.9 ppm (s, 1H); IR (KBr): ν = 3230, 2110, 1690, 1300, 1165 cm^{-1}; MS (EI, 70 eV): *m/z*: 346 $[M]^+$.

2.1.5 General Procedures for Synthesizing 9-(R)-6,11-dihydrodibenzo[c,f][1,2,5]thiadiazepine-5,5-dioxide (2a–2f)

2-azido-*N*-(4-(R)phenyl) benzenesulfonamide **4** (0.2 g, 0.73 mmol) was added to a solution of diphenyl ether (10 mL, 63 mmol) at 208 °C. The solution was stirred for 5 min then cooled to room temperature. The reaction mixture was purified by flash chromatography (70:30, ethyl acetate–hexane). The resulting residue was recrystallized in ethyl acetate–hexane (30:70).

Compounds **2a** and **2d** were previously reported by Altamura et al. (Altamura et al., 2009), and spectroscopic data are in agreement with those reported here.

6,11-dihydrodibenzo[*c*,*f*][1,2,5]thiadiazepine-5,5-dioxide (2a): Brown crystals (0.50 mmol, 69%); mp: 198 ºC; ^{1}H NMR (300 MHz, [D$_6$]DMSO): *d* = 6.82 (ddd, J_o= 7.8 Hz, J_m= 0.9 Hz, 1H), 6.88 (dd, J_o= 7.4 Hz, J_m= 1.5 Hz, 1H), 7.03 (ddd, J_o= 7.7 Hz, J_m= 1.5 Hz, 1H), 7.07 (dd, J_o= 8.1 Hz, J_m= 1.5 Hz, 1H), 7.14 (ddd, J_o= 7.5 Hz, J_m= 1.5 Hz, 1H), 7.18 (dd, J_o= 8.2 Hz, J_m= 1.0 Hz, 1H), 7.37 (ddd, J_o= 7.7 Hz, J_m= 1.6 Hz, 1H), 7.61 (dd, J_o= 8.0 Hz, J_m= 1.6 Hz, 1H), 8.98 (s, 1H), 9.80 ppm (s, 1H); ^{13}C NMR (75 MHz, [D$_6$]DMSO): *d* = 117.5, 119.5, 119.6, 121.1, 125.2, 125.9, 127.3, 128.4, 128.8, 132.9, 139.5, 139.9 ppm; IR (KBr): ν = 3380, 3301, 1313, 1160 cm^{-1}; MS (EI, 70 eV): *m/z*: 246 [M]$^{+}$; Anal. calculated for $C_{12}H_{10}N_2O_2S$: C 58.52%, H 4.09%, N 11.37%, found: C 58.11%, H 4.11%, N 11.13%.

9-fluoro-6,11-dihydrodibenzo[*c*,*f*][1,2,5]thiadiazepine-5,5-dioxide (2b): Colorless needle crystals. Yield 70%; mp: 202 ºC; ^{1}H NMR (300 MHz, [D$_6$]DMSO): *d* = 6.69 (ddd, J_o= 8.2 Hz, $J_{mH\text{-}F}$ = 3.0 Hz, 1H), 6.86 (dd, J_o= 7.2 Hz, 1H), 6.89 (d, J_m= 2.7 Hz, 1H), 7.05 (dd, J_o= 7.5 Hz, 1H), 7.16 (dd, J_o= 8.1 Hz, J_m= 0.6 Hz, 1H), 7.41 (ddd, J_o= 7.6 Hz, J_m= 1.5 Hz, 1H), 7.63 (dd, J_o= 8.0 Hz, J_m= 1.8 Hz, 1H), 9.14 (s, 1H), 9.78 ppm (s, 1H); ^{13}C NMR (75 MHz, [D$_6$]DMSO): *d* = 105.6, 107.6, 119.0, 121.4, 126.1, 129.3, 130.4, 133.1, 139.2, 141.3, 159.2, 162.5 ppm; IR (KBr): ν = 3365, 3226, 1295, 1159 cm^{-1}; MS (EI, 70 eV): *m/z*: 264 [M]$^{+}$; Anal. calculated for $C_{12}H_9N_2O_2SF$: C 54.54%, H 3.43%, N 10.60%, found: C 54.05%, H 3.32%, N 10.34%.

9-chloro-6,11-dihydrodibenzo[*c*,*f*][1,2,5]thiadiazepine-5,5-dioxide (2c): White powder. Yield 79%; mp: 248 ºC; ^{1}H NMR (300 MHz, [D$_6$]DMSO): *d* = 6.87 (ddd, J_o= 7.8 Hz, J_m= 1.2 Hz, 1H), 6.88 (dd, J_o= 8.4 Hz, J_m= 2.1 Hz, 1H), 7.01 (d, J_o= 8.4 Hz, 1H), 7.13 (d, J_m= 2.1 Hz, 1H), 7.15 (dd, J_o= 8.1 Hz, J_m= 0.6 Hz, 1H), 7.41 (ddd, J_o= 7.7 Hz, J_m= 1.5 Hz, 1H), 7.62 (dd, J_o= 8.0 Hz, J_m= 1.6 Hz, 1H), 9.11 (s, 1H), 9.95 ppm (s, 1H); ^{13}C NMR (75 MHz, [D$_6$]DMSO): *d* = 118.3, 118.7, 119.7, 120.4, 124.2, 125.8, 129.2, 129.5, 131.1, 133.3, 139.2, 140.5 ppm; IR (KBr): ν = 3369, 3269, 1304, 1156 cm^{-1}; MS (EI, 70 eV): *m/z*: 280 [M]$^{+}$; Anal. calculated for $C_{12}H_9N_2O_2SCl$: C 51.34%, H 3.23%, N 9.98%, found: C 51.03%, H 3.22%, N 9.81%.

9-bromo-6,11-dihydrodibenzo[*c*,*f*][1,2,5]thiadiazepine-5,5-dioxide (2d): Brown powder. Yield 85%; mp: 250 ºC; ^{1}H NMR (300 MHz, [D$_6$]DMSO): *d* = 6.87 (ddd, J_o= 7.4 Hz, 1H), 6.94 (d, J_o= 8.4 Hz, 1H), 7.01 (dd, J_o= 8.2 Hz, J_m= 2.0 Hz, 1H), 7.15 (d, J_o= 8.4 Hz, 1H), 7.28 (d, J_m= 1.8 Hz, 1H), 7.41 (ddd, J_o= 7.8 Hz, 1H), 7.62 (dd, J_o= 7.8 Hz, J_m= 1.2 Hz, 1H), 9.10 (s, 1H), 9.96 ppm (s, 1H); ^{13}C NMR (75 MHz, [D$_6$]DMSO): *d* = 118.3, 119.2, 119.7, 121.6, 123.3, 124.6, 125.8, 129.2, 129.7, 133.3, 139.2, 140.7 ppm; IR (KBr): ν = 3371, 3268, 1308, 1160 cm^{-1}; MS (EI, 70 eV): *m/z*: 326/324 [M]$^{+}$; Anal. calculated for $C_{12}H_9N_2O_2SBr$: C 44.32%, H 2.79%, N 8.61%, found: C 44.09%, H 2.81%, N 8.74%.

9-methoxy-6,11-dihydrodibenzo[*c*,*f*][1,2,5]thiadiazepine-5,5-dioxide (2e): Yellow crystals. Yield 67%; mp: 171 ºC; ^{1}H NMR (300 MHz, [D$_6$]DMSO): *d* = 3.73 (s, 3H), 6.49 (dd, J_o= 8.7 Hz, J_m= 2.7 Hz, 1H), 6.66 (d, J_m= 2.7 Hz, 1H), 6.83 (ddd, J_o= 7.5 Hz, J_m= 0.9 Hz, 1H), 6.96 (d, J_o= 8.7 Hz, 1H), 7.17 (d, J_o= 7.8 Hz, 1H), 7.37 (ddd, J_o= 7.7 Hz, J_m= 1.5 Hz, 1H,), 7.62 (dd, J_o= 7.8 Hz, J_m= 1.5 Hz, 1H), 8.99 (s,

1H), 9.51 ppm (s, 1H); ^{13}C NMR (75 MHz, [D$_6$]DMSO): *d* = 55.2, 104.2, 107.4, 117.7, 118.1, 119.5, 126.3, 129.0, 130.4, 132.8, 139.7, 141.2, 158.6 ppm; IR (KBr): ν = 3374, 3228, 1322, 1149 cm^{-1}; MS (EI, 70 eV): *m/z*: 276 [M]$^+$; Anal. calculated for $C_{13}H_{12}N_2O_3S$: C 56.51%, H 4.38%, N 10.14%, found: C 56.56%, H 4.40%, N 9.89%.

Ethyl 6,11-dihydrodibenzo[*c*,*f*][1,2,5]thiadiazepine-9-carboxylate-5,5-dioxide (2f): Brown crystals. Yield 12%; mp: 227 ºC; ^{1}H NMR (300 MHz, [D$_6$]DMSO): *d* = 1.31 (t, J_o= 7.0 Hz, 3H), 4.30 (q, J_o= 7.2 Hz, 2H), 6.85 (ddd, J_o= 7.5 Hz, 1H), 7.07 (d, J_o= 8.1 Hz, 1H), 7.19 (d, J_o= 7.8 Hz, 1H), 7.40 (dd, J_o= 8.1 Hz, 1H), 7.40 (ddd, J_o= 7.6 Hz, 1H), 7.61 (dd, J_o= 7.8 Hz, J_m= 1.5 Hz, 1H), 7.73 (d, J_m= 1.8 Hz, 1H), 9.20 (s, 1H), 10.3 ppm (s, 1H); ^{13}C NMR (75 MHz, [D$_6$]DMSO): *d* = 14.2, 60.7, 118.1, 119.6, 120.4, 121.3, 125.3, 126.8, 128.2, 128.9, 129.6, 133.4, 138.3, 139.6, 165.1 ppm; IR (KBr): ν = 3360, 3234, 1700, 1328, 1170 cm^{-1}; MS (EI, 70 eV): *m/z*: 318 [M]$^+$; Anal. calculated for $C_{15}H_{14}N_2O_4S$: C 56.59%, H 4.43%, N 8.80%, found: C 56.67%, H 4.44%, N 8.64%.

Procedures for Synthesizing 6,11-dihydrodibenzo[c,f][1,2,5]thiadiazepine-9-carboxylic acid 5,5-dioxide (2g)

A solution of potassium hydroxide 10% (w/v) was added to ethyl 6,11-dihydrodibenzo[*c*,*f*][1,2,5]thiadiazepine-9-carboxylate-5,5-dioxide **2f** (0.5 g, 1.57 mmol). The reaction mixture was heated under reflux and stirred for 60 min, after which a chloride acid solution was added to a pH of 6. The resulting solid was collected, washed with water, and dried under vacuum. The resulting yellow solid residue was obtained in a quantitative yield; mp: 350 °C; ^{1}H NMR (300 MHz,

[D_6]DMSO): *d* = 6.84 (ddd, J_o= 7.6 Hz, J_m= 1.0 Hz, 1H), 7.05 (d, J_o= 8.1 Hz, 1H), 7.18 (d, J_o= 8.1 Hz, 1H), 7.39 (dd, J_o= 8.1 Hz, J_m= 1.8 Hz, 1H), 7.39 (ddd, J_o= 7.6 Hz, J_m= 1.8 Hz, 1H), 7.61 (dd, J_o= 8.0 Hz, J_m= 1.6 Hz, 1H), 7.72 (d, J_m= 1.8 Hz, 1H), 9.15 (s, 1H), 10.7 ppm (s, 2H); ^{13}C NMR (75 MHz, [D_6]DMSO): *d* = 118.0, 119.6, 120.7, 121.6, 125.4, 126.8, 128.9, 129.3, 129.4, 133.4, 138.3, 139.7, 166.7 ppm; IR (KBr): ν = 3360, 3234, 1700, 1328 cm^{-1}; MS (EI, 70 eV): *m/z*: 290 [M]$^+$; Anal. calculated for $C_{13}H_{10}N_2O_4S$: C 53.79%, H 3.47%, N 9.65%, found: C 53.73%, H 3.47%, N 9.28%.

2.2 Biological Methods

2.2.1 Primary Cultures of the Myenteric Neurons

Guinea pigs (100–200 g; either male or female) were sacrificed by cervical dislocation and carotid exsanguination. These methods have been approved by the Animal Care Committee of the IPICYT and are in agreement with the published Guiding Principles in the Care and Use of Animals, approved by the American Physiological Society. A segment of ~10 cm of the jejunum was removed and placed in a modified Krebs solution (in mM: NaCl, 126; NaH_2PO_4, 1.2; $MgCl_2$, 1.2; $CaCl_2$, 2.5; KCl, 5; NaH_2CO_3, 25; glucose, 11. The sample was gassed under 95% O_2 and 5% CO_2) and opened longitudinally. A dissecting microscope was used to dissect the mucosa and submucosa layers prior to removing most of the circular muscle layer, leaving the myenteric plexus embedded in a longitudinal layer.

The cell isolation procedure has been described elsewhere (Barajas-Lopez et al., 1996). The myenteric preparation was dissociated by sequential treatment

with two enzymatic solutions: the first solution contained papain (0.01 mL mL^{-1} activated with 0.4 mg mL^{-1} L-cysteine), and the second solution contained collagenase (1 mg mL^{-1}) and dispase (4 mg mL^{-1}). The enzymes were removed by washing the neurons with L15 medium, and the neurons were placed on round coverslips coated with sterile rat-tail collagen. The culture medium was varied from minimal medium to essential medium 97.5% containing 2.5% guinea pig serum, 2 mM L-glutamine, 10 $U \cdot mL^{-1}$ penicillin, 10 $\mu g \cdot mL^{-1}$ streptomycin, and 15 mM glucose.

2.2.2 Whole-Cell Recordings of the Membrane Currents Induced by GABA

To reduce the effects of the membrane currents other than those mediated by the activation of LGIC, experiments were conducted in the presence of Cs^+ (a potassium channel blocker). This was important because GABA modulates the membrane ion channels of the central neurons (enteric neurons) via G-protein linked receptors (Cherubini and North, 1984; Krantis, 2000; Wellendorph and Brauner-Osborne, 2009). Membrane currents induced by GABA were recorded using a Gene Clamp 500B amplifier (Axon Instruments, Inc.). The holding potential was −60 mV (unless otherwise stated), and the short-term (4–50 h) primary cultures of the myenteric neurons were used to prevent space-clamp problems due to neurite growth. Glass pipettes with a resistance of 2–5 MΩ were prepared as described previously (Barajas-Lopez et al., 1996). This low resistance and slight suction inside the pipette during the recordings maintained a low series resistance (around 6 MΩ).

All experiments were conducted using standard solutions with the following compositions (in mM); inside the pipette: CsCl, 160; EGTA, 10; HEPES, 5; NaCl, 10; ATPMg, 3 and GTP, 0.1; external solution: NaCl, 160; $CaCl_2$, 2; glucose, 11; HEPES, 5 and CsCl, 3. The pH of all solutions was adjusted to 7.3–7.4 using either CsOH (pipette solution) or NaOH (external solution). The seal resistance in the whole-cell mode ranged from 1 to 10 GW. The whole-cell current data were recorded on a PC using the AxoScope software (Axon Instruments, Inc.) and were analyzed using the AXOGRAPH software (Molecular devices). The recording chamber was superfused with an external solution at ~2 mL min^{-1}. The solution around the neuron was quickly exchanged during recordings using an eight-tube device. Each tube was connected to a syringe (10 mL) containing either the control or the experimental solution. A control tube was positioned ~300 µm in front of the recorded neuron, and substances were applied externally by abruptly interchanging the tube for another tube containing the control solution plus the drug(s). Desensitization of the $GABA_A$ receptors was prevented by applying GABA at intervals of at least 5 min, in between cells were continuously superfused with extracellular solution. Experimental substances were removed by returning to the control solution. External solutions were applied by gravity, and the height of the syringes was continuously adjusted to minimize changes in the flow rate. The experiments were performed at room temperature (24 ± 1 °C).

2.2.3 Solutions and Reagents

L15 medium, minimum essential medium, Hanks solution, penicillin-streptomycin, and L-glutamine were purchased from GIBCO. Collagenase and papain were

purchased from Worthington, and dispase was purchased from Roche. Cesium chloride, sodium chloride, ethylene glycol-bis(2-aminoethylether)-*N,N,N′,N′*-tetra-acetic acid (EGTA), HEPES, adenosine-5′-triphosphate magnesium salt (ATP magnesium salt), guanosine-5′-triphosphate sodium salt (GTP sodium salt), cesium hydroxide, flumazenil, GABA, picrotoxin, and dimethyl sulfoxide were purchased from Sigma-Aldrich (St. Louis, MO, USA). Picrotoxin and the DBTD stock solutions, which were prepared in ethanol (50% v/v) and DMSO, respectively. The desired final drug concentration was obtained by diluting the stock solutions in an external solution prior to application.

2.2.4 Data Analysis

The concentration–response data were fit to a logistic model: $I = I_{max}/[1+(EC_{50}/[A])^{nH}]$, where [A] is the agonist concentration, I is the current, and I_{max} is the maximum current. EC_{50} is the concentration of drug that elicits a half-maximum response, and nH is the Hill coefficient. Experimental data were reported as ± SEM, and n represents the number of cells used. The unpaired Student's t-test was applied to data obtained from two different groups of cells. One-way ANOVA and the Bonferroni tests were used to compare multiple means. The two-tailed *P* values of 0.05 or less were considered to be statistically significant.

2.2.5 Theoretical calculations

Quantum chemical calculations of the DBTDs structures **2a**–**2g** in the gas phase were performed using GAUSSIAN 03 (Frisch et al., 2004) in conjunction with density functional theory (DFT) calculations. Geometry optimization of the DBTDs

was followed by frequency calculations performed at the B3LYP/6-311 ++G(d,p) level. Table 1 reports the cLog *P*, generated using HyperChem, of each optimized structure obtained from Gaussian V03.

CHAPTER 3 RESULTS AND DISCUSSION

3.1 Synthesis of DBTDs

The synthetic route begins with the reaction of 4-substituted-anilines with 2-nitrobenzenesulfonyl chloride under reflux using pyridine as the base and acetone as solvent. The 2-nitrosulfonamides **5a–5f** were obtained in good yields (66–88%). The subsequent catalytic hydrogenation of the nitro group using dehydrated tin(II) chloride under reflux with ethyl acetate yielded the amines **6a–6f** in yields above 88%. The amino compounds were transformed to the corresponding 2-azidobenzensulfonamides through their diazotization with sodium nitrite in trifluoroacetic acid. (Note that the transformation of **6e** was accomplished using hydrochloric acid). The in situ substitution of the diazo group with sodium azide induced conversion to **4a–4f** with a 78–87% yield. In the final step, the thiadiazepine formation reaction proceeded via thermolysis above 208 °C in diphenyl ether, this temperature favored the formation of an intermediate nitrene reagent (Jian and Tour, 2003). A direct N-C-type amination of the C ring provided the DBTDs **2a–2f** with yields of 67–85%, except for compound **2f**, which was isolated with a yield of 12%. Compound **2g** was obtained by basic hydrolysis of **2f** after a hydrochloride acid treatment.

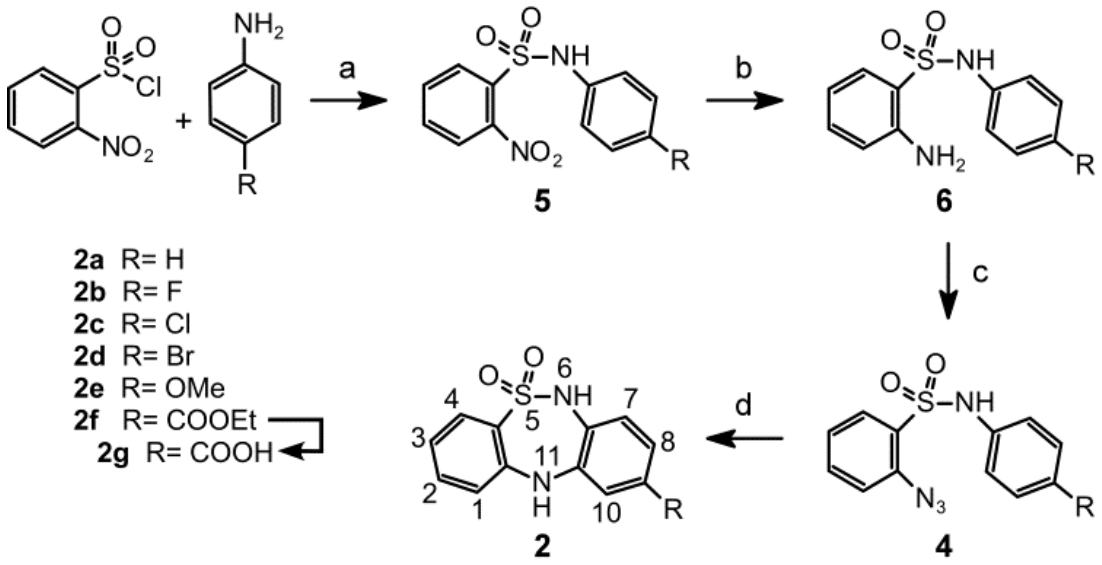

Scheme 1. Reagents and conditions: a) Anhydrous pyridine, dry acetone, $N_{2(g)}$, 24 h; b) $SnCl_2.2H_2O$, ethyl acetate, 4 h; c) first step: $NaNO_2$, F_3CCO_2H, 1 h; second step: NaN_3, 1 h; d) $(C_6H_5)_2O$, 208 °C, 5 min. 2g was obtained from 2f: first step: KOH 10%, 1 h; second step: HCl 10%.

3.2 Pharmacological Analysis on $GABA_A$ Receptors

The inhibitory effects of DBTDs on the native $GABA_A$ receptors of guinea pig myenteric neurons were studied here for the first time. The Cl^- concentrations outside and inside the neurons were similar, and a holding potential was −60 mV. At this potential, GABA (0.03–3 mM) induced inward currents (I_{GABA}) in 86% of myenteric neurons. The amplitude of the currents was concentration-dependent (EC_{50} = 115 ± 10 μM) and varied among the different neurons with an amplitude range of 0.1–6 nA in response to 300 μM GABA. Most neurons maintained a stable value of I_{GABA} during repeated GABA applications. Otherwise, the data were rejected. In order to test that these GABA currents are mediated by $GABA_A$ channels bicuculline (0.1–100 μM) and picrotoxin (3–1000 μM) were used, inhibitors of these receptors (Karanjia et al., 2006; Miranda-Morales et al., 2007; Zhou and Galligan, 2000). Both substances inhibited I_{GABA} in a concentration-dependent manner (data not shown) with an IC_{50} of 10±2 and 6±1 μM, respectively. Maximal concentrations used for both antagonists virtually abolished I_{GABA}, as it was previously reported (Karanjia et al., 2006; Miranda-Morales et al., 2007; Zhou and Galligan, 2000).

Figure 4 shows that the DBTDs (100 μM) inhibited the currents induced by GABA (300 μM) in a time-dependent manner (3–180 s) with time constants (*t*) of 4.9, 2.6, and 29.3 s for **2b**, **2c**, and **2d**, respectively. These constants were calculated by fitting the data using the Michaelis–Menten equation (R^2 = 0.98, 0.88, and 0.99, respectively). The maximum inhibition induced by **2b** and **2c** (100 μM) was reached 3 min after initial exposure. For **2d,** the time required to reach the

maximum inhibition was calculated to be 17 min; however, the experimental maximum inhibition observed after a 3 min treatment was 74.2 ± 2.4% (n=10), similar to the calculated maximum inhibition, 87.0 ± 3.0%. In all subsequent experiments, a DBTD treatment time of 3 min was used. The current inhibition induced by **2b**, **2c**, and **2d** was fully reversed within five minutes of washing. The holding current remained constant in the presence of the compounds at all concentrations tested, indicating that the compounds could not open the $GABA_A$ receptors or any other neuronal ion channel under the experimental conditions.

Control experiments were conducted using DMSO, the solvent used for all DBTDs, demonstrating that DMSO did not modify the properties of I_{GABA} alone at the maximum concentration used here, 0.33% V/V (data not shown). The inhibitory activities of the DBTDs were likely to be use-independent because the compounds effects did not require active $GABA_A$ receptors and the inhibitory activity increased over time, despite the absence of the agonist (GABA) (Krehan et al., 2006). This indicates that DBTDs bind to the closed stage of these channels.

The inhibitory effects of seven DBTDs at a 100 µM concentration are listed in Table 1. The data indicate that the rank order of potency for these inhibitors was **2c** = **2d** > **2b** = **2f** = **2e** > **2a** > **2g**. Figure 5 shows the concentration–response curves for the inhibitory effects of three DBTDs (3–1000 µM) on the currents induced by GABA (300 µM). The maximum effect of **2b** was achieved at 1 mM, yielding complete inhibition of the GABA-activated inward currents; with an IC_{50} value (104 ± 9.2 µM). We did not reach the maximum inhibition for **2c** and **2d** because the compounds were insoluble at concentrations exceeding 300 µM under

our experimental conditions. Curve fits were obtained in both cases with IC_{50} values of 50.4 ± 6.4 µM and 47.6 ± 30.3 µM for **2c** and **2d**, respectively.

Table 1. Percent inhibition in the presence of 100 µM compounds on GABA-induced inward currents, p IC_{50}, log *P*, and physical data.

No.	Percentage of inhibition[a]	p IC_{50} / M	log *P*[b]	Yield / %	mp / °C
2a	28.4 ± 1.4 (5)	ND	2.18	69	198
2b	50.8 ± 2.1 (12)	3.98	1.50	70	202
2c	74.2 ± 3.6 (6)	4.30	2.69	79	248
2d	74.2 ± 2.4 (10)	4.32	2.97	85	250
2e	43.7 ± 3.8 (3)	ND	1.92	67	171
2f	47.1 ± 3.7 (7)	ND	2.25	12	227
2g	16.0 ± 2.4 (6)	ND	1.87	100	350

[a] Values are given as the mean ± SEM, with the number of experiments in parentheses. [b] Data generated using HyperChem.

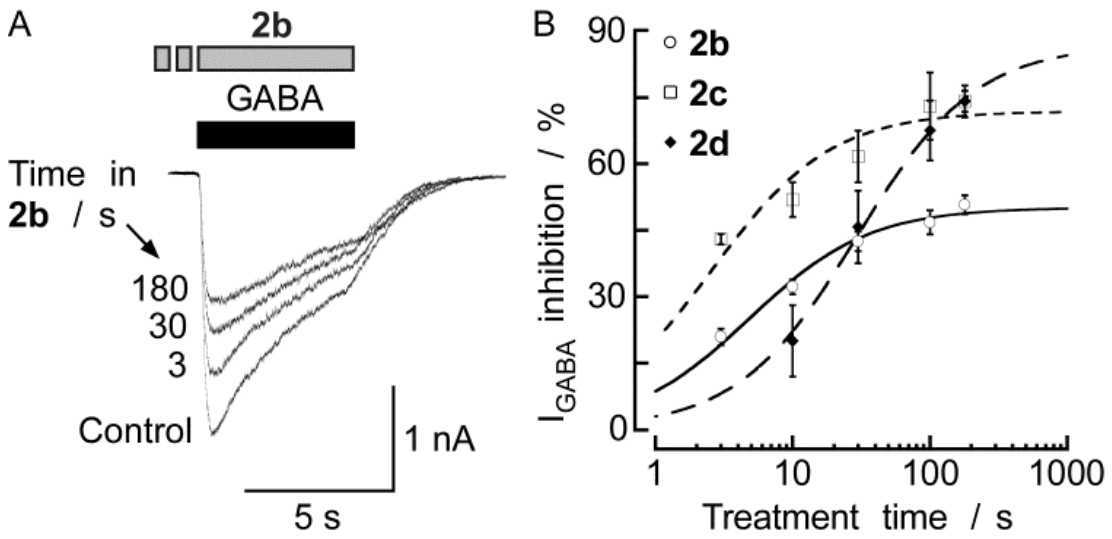

Figure 4. Halogenated DBTDs inhibited the I_{GABA} in a time-depended manner. A) I_{GABA} was recorded before, during application of 100 μM **2b**, and after removal of the inhibitor of a given myenteric neuron for various lengths of time. The horizontal bars above the traces indicate the application profiles of the indicated substances. B) Time course of I_{GABA} (induced by 300 μM GABA) inhibition induced by **2** over 3–180 s. Michaelis–Menten fits. Each data point represents the mean value from 3–12 different experiments. The lines represent the SEM.

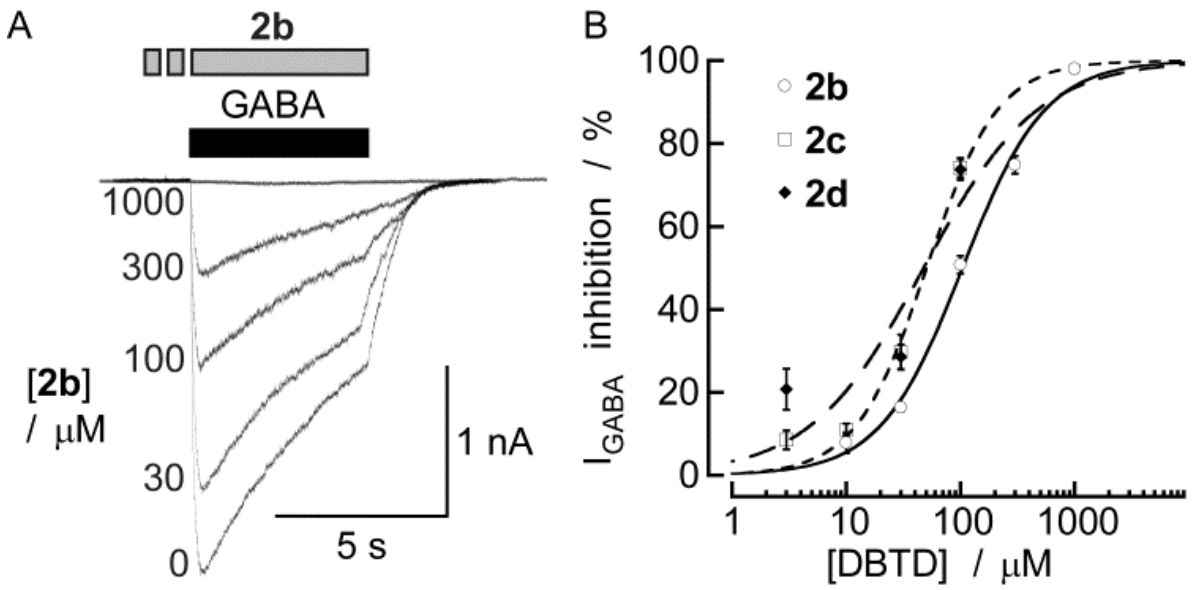

Figure 5. DBTDs inhibited I_{GABA} in a concentration-dependent manner. A) Representative I_{GABA} recordings from a myenteric neuron in the presence of various concentrations of **2b**, which was added 3 min before GABA application. B) Concentration–response curves for the effects of the DBTDs on the amplitude of I_{GABA}. The lines indicate fits to the experimental data using a two-parameter logistic function (Kenakin, 1993), assuming an inhibition of 100%. Each data point represents the mean ± SEM from 3–12 individual experiments.

We considered the possibility that because these novel substances were highly lipophilic (log *P* ~ 2.0 for all compounds, Table 1), the DBTDs could permeate the neuron membrane and interact with the inner part of the $GABA_A$ channel, thereby inhibiting I_{GABA}. To investigate this possibility, we added 100 μM **2b** to the pipette solution (internal) and monitored I_{GABA}, and we applied **2b** to the outside of the cells and monitored the inhibitory effects (Figure 6). Experiments were performed using **2b**, even though cLog *P* was less than 2, because **2c** and **2d** were insoluble under the conditions employed. The amplitude of I_{GABA} (300 μM) for neurons with **2b** (100 μM) applied inside (−1408 ± 344 pA; n=4) and measured 2 to 3 min after obtaining the whole cell configuration did not differ from the amplitude of the control I_{GABA} (−1510 ± 333 pA; n=12) of experiments in which **2b** was tested extracellularly. Consistent with these findings, in recordings with **2b** in the pipette, the amplitude of I_{GABA} was the same 5 min (−1536 ± 379 pA) and 10 min (−1604 ± 409 pA; n=4) after obtaining the whole-cell configuration. In addition, the presence of **2b** inside the neurons did not affect the magnitude of the inhibition induced by the extracellular application of **2b** (100 μM). Thus, such an inhibition was as large as that observed without **2b** inside the cells (Figure 6B). Altogether, these data rule out that DBTDs inhibitory effect on $GABA_A$ channels are mediated by an intracellular target and they must be binding to an extracellular region of the channels.

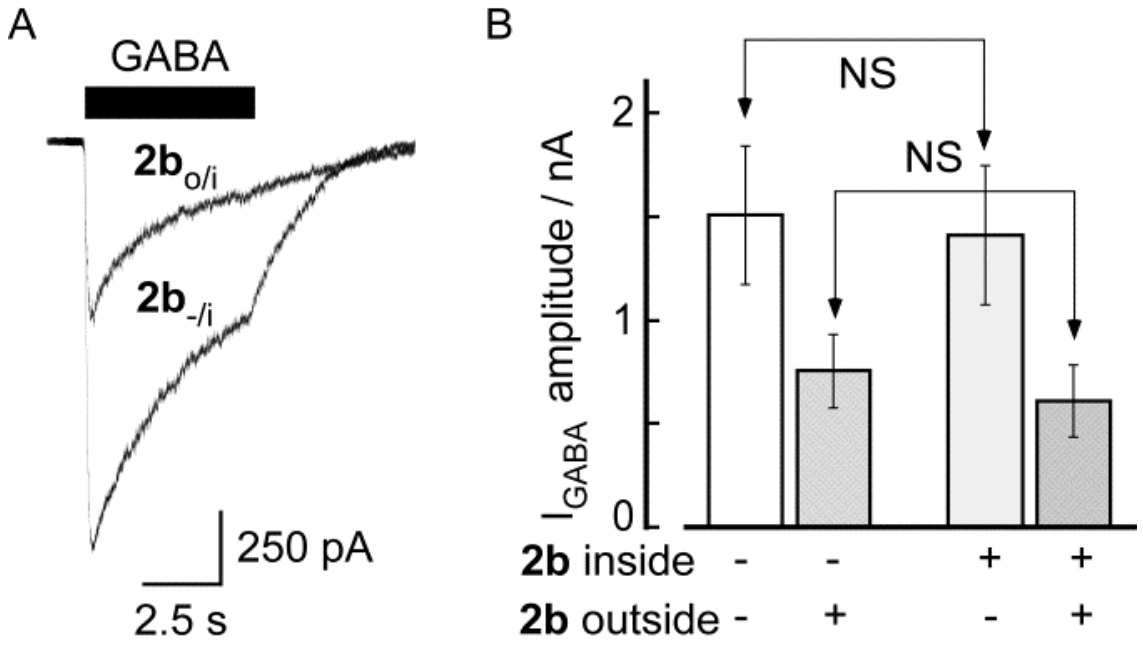

Figure 6. The inhibitory effects of **2b** on $GABA_A$ receptors were mediated by an extracellular binding site. A) I_{GABA} for a 100 µM concentration of **2b** in the pipette (**2b**$_{-/i}$), 10 min after obtaining the whole cell. I_{GABA} was recorded before (-/i) and in presence of extracellular (o/i) **2b** (100 µM for 3 min). B) Bars indicate the average amplitude of I_{GABA}, and the lines above indicate the SEM. I_{GABA} amplitude or the inhibitory effect of **2b** did not differ significantly (NS) by the presence of **2b** inside the pipette. Statistical comparison of the data was done using the unpaired Student's *t*-test.

Figure 7 shows two concentration-response curves for the effects of GABA, one in the absence and the other in the presence of 100 µM **2b**. As shown, the antagonistic effect of **2b** is not surmounted by increasing the GABA concentration. Indeed, the EC_{50} values for these curves were 126.7 ± 16 and 123.4 ± 84 µM in the absence and in the presence of **2b**, whereas, the maximum inhibition clearly decreased in the presence of **2b** (~50%) across the full GABA concentration–response curve. Our data demonstrate that the pharmacological antagonism by which **2b** inhibits the $GABA_A$ receptors is non-competitive and therefore, it is unlikely acting at the GABA binding site.

The tricyclic sulfonamide **2** is also structurally similar to the 1,4-benzodiazepines, hence, DBTD inhibitory actions may be related to the benzodiazepine modulator sites. The inhibitory effects of **2b**, **2c**, and **2d** remained constant in the absence and presence of flumazenil, a known antagonist of the benzodiazepine site on the $GABA_A$ receptors (Figure 8). Inhibition by 100 µM **2b**, **2c**, and **2d** without flumazenil (50.8 ± 2.1%, 74.2 ± 3.6%, 74.2 ± 2.4%, respectively) was not blocked by the co-application of 10 µM flumazenil (47.8 ± 5.8%, 69.6 ± 5.2%, 68.4 ± 6.8%, respectively). The same concentration of flumazenil, applied for 3 min, did not induce changes in the holding current or I_{GABA} in experiments carried out using five different neurons (Data not shown). We showed that **2b** did not act through the benzodiazepine binding site, which is in agreement with the lack of binding with receptors to benzodiazepine, previously reported (Giannotti et al., 1991).

We further investigated if the inhibitory effect of DBTD on I_{GABA} was voltage dependent by conducting experiments at two holding membrane potentials, −60 mV and +40 mV in the same neurons. I_{GABA} (300 μM) was recorded in the absence or presence of 100 μM **2b**, **2c**, and **2d**. As shown in Figure 9, the inhibitory effects induced by any of the three substances were identical for an inward I_{GABA} (recorded at −60 mV) than for the outward I_{GABA} (recorded at +40 mV). These results suggested that the DBTDs affected the I_{GABA} via a voltage-independent mechanism.

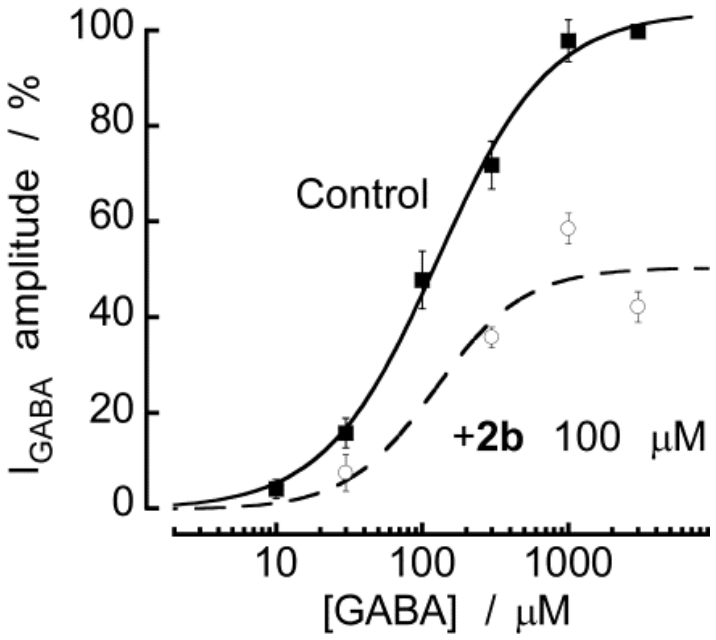

Figure 7. 2b inhibits I_{GABA} in a non-competitive manner. A) Concentration–response curves for GABA in the absence (Control) and in the presence of **2b**. Responses were normalized with respect to the curves obtained in the presence of 3 mM GABA in each cell and in the absence of **2b**. Each point represents the mean ± SEM for 5–12 neurons. The lines indicate fits of experimental data to a three-parameter logistic function.

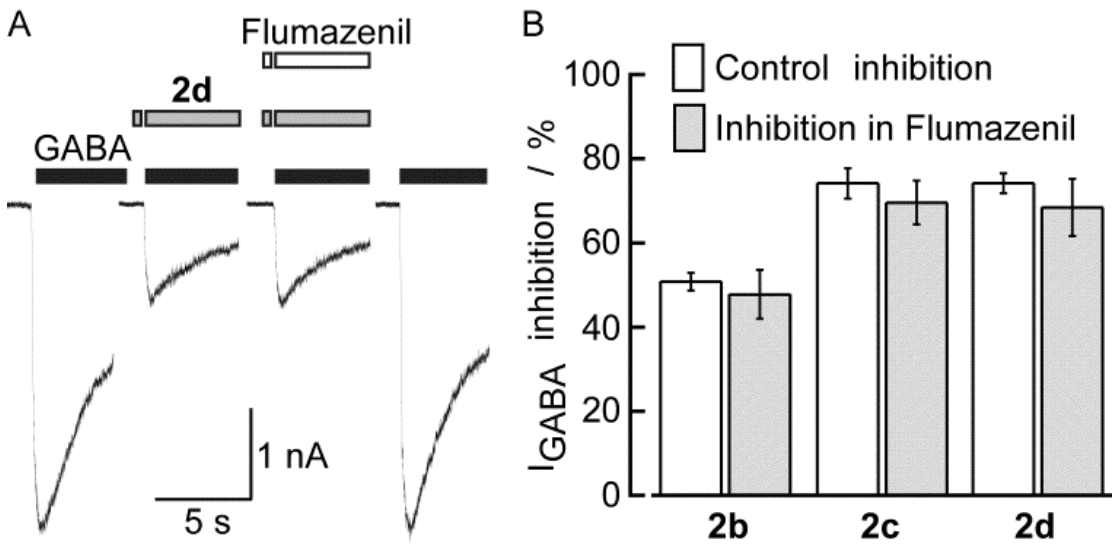

Figure 8. The inhibitory effects of compounds **2** on the $GABA_A$ channels were independent of the benzodiazepine binding site. A) First and last traces represent control currents induced by GABA (300 µM). The two middle traces were recorded in **2d** (100 µM) alone or plus flumazenil (10 µM), all traces are from the same neuron. B) Each pair of bars represents the mean inhibition of I_{GABA} induced by DBTDs, before (Control) and in the presence of flumazenil. Lines over the bars indicate the SEM.

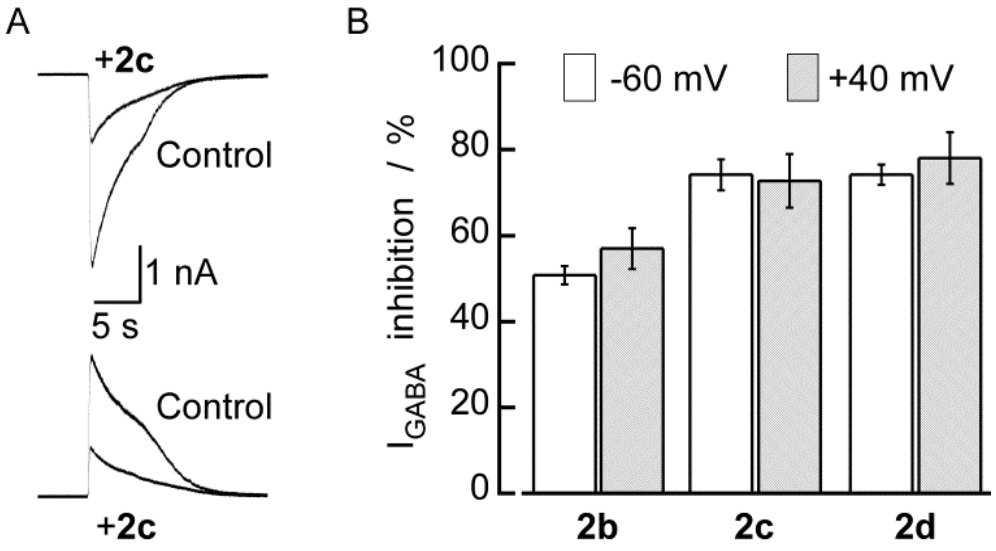

Figure 9. The inhibitory effects of compounds **2** on $GABA_A$ channels were voltage independent. A) I_{GABA} induced by 300 µM GABA without (Control) or in presence of **2c** (100 µM) at −60 mV (upper traces) and +40 mV (lower traces) from the same neuron. I_{GABA} was recorded at 5 min intervals, and **2c** was applied 3 min before the second GABA application. B) The average (bars) inhibitory effect of **2b**, **2c**, and **2d** was the same at both membrane potentials. Lines over the bars indicate the SEM.

The fact that binding of compounds **2** on $GABA_A$ channels can occur during the close stage and is voltage independent suggests that its binding site is not within the channel pore. In order to further study this, we investigate if picrotoxin interacts with the binding of **2c**. Picrotoxin is known to bind into a site within the channel formed by the second transmembrane domains of the five subunits constituting the $GABA_A$ receptors (Olsen, 2006; Sieghart et al., 2012). We found that neither picrotoxin effect was modified by **2c** nor the inhibitory effect of **2c** was affected by picrotoxin (Figure 10), which would indicate that **2c** does not bind into the picrotoxin binding site.

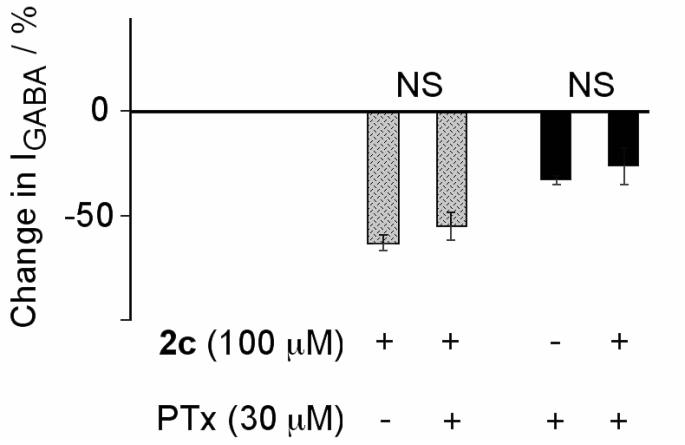

Figure 10. The inhibitory effects of compounds **2** on the $GABA_A$ channels were independent of the benzodiazepine binding site. A) First and last traces represent control currents induced by GABA (300 μM). The two middle traces were recorded in **2d** (100 μM**)** alone or plus flumazenil (10 μM), all traces are from the same neuron. B) Each pair of bars represents the mean inhibition of I_{GABA} induced by DBTDs, before (Control) and in the presence of flumazenil. Lines over the bars indicate the SEM.

CONCLUSIONS

We described the preparation of novel DBTDs via a nitrene radical that inserted into the C on the aromatic ring. Seven derivatives were generated (**2a–g**), and their effects on $GABA_A$ neuronal receptors were tested. The DBTDs inhibited I_{GABA} in a time- and concentration-dependent manner.

The DBTDs displayed an inhibitory effect on the $GABA_A$ channel of myenteric neurons, and this antagonism was non-competitive indicating that it does not bind to the GABA receptor and their effect is likely allosteric. Inhibition was mediated by an extracellular binding site that was most likely not in the mouth of the channel and therefore, it is unlikely that this effect is mediated by channel blockage. Their effect was also independent of the benzodiazepine binding site. The DBTDs described here could be used as a model to explore new $GABA_A$ receptor inhibitors with a potential to be used as antidotes for substances known to positively modulate $GABA_A$ channel activity or as a new drugs to induce experimental epilepsy. These compounds appear to bind on a different site than picrotoxin; therefore, they could be used alone or in combination with picrotoxin. Future experiments will be aimed to molecularly identify DBTDs binding sites on $GABA_A$ receptors.

BIBLIOGRAPHY

Altamura M, Fedi V, Giannotti D, Paoli P and Rossi P (2009) Privileged structures: synthesis and structural investigations on tricyclic sulfonamides. *New J Chem* **33**(11):2219-2231.

Barajas-Lopez C, Peres AL and Espinosa-Luna R (1996) Cellular mechanisms underlying adenosine actions on cholinergic transmission in enteric neurons. *Am J Physiol* **271**(1 Pt 1):C264-275.

Bellarosa D, Antonelli G, Bambacioni F, Giannotti D, Viti G, Nannicini R, Giachetti A, Dianzani F, Witvrouw M, Pauwels R, Desmyter J and De Clercq E (1996) New arylpyrido-diazepine and -thiodiazepine derivatives are potent and highly selective HIV-1 inhibitors targeted at the reverse transcriptase. *Antiviral Res* **30**(2-3):109-124.

Brickley SG and Mody I (2012) Extrasynaptic GABA(A) receptors: their function in the CNS and implications for disease. *Neuron* **73**(1):23-34.

Brookes SJ (2001) Classes of enteric nerve cells in the guinea-pig small intestine. *Anat Rec* **262**(1):58-70.

Cherney RJ, Duan JJW, Voss ME, Chen LH, Wang L, Meyer DT, Wasserman ZR, Hardman KD, Liu RQ, Covington MB, Qian MX, Mandlekar S, Christ DD, Trzaskos JM, Newton RC, Magolda RL, Wexler RR and Decicco CP (2003) Design, synthesis, and evaluation of benzothiadiazepine hydroxamates as selective tumor necrosis factor-alpha converting enzyme inhibitors. *J Med Chem* **46**(10):1811-1823.

Cherubini E and North RA (1984) Actions of gamma-aminobutyric acid on neurones of guinea-pig myenteric plexus. *Br J Pharmacol* **82**(1):93-100.

Cooke HJ (1998) "Enteric Tears": Chloride Secretion and Its Neural Regulation. *News Physiol Sci* **13**:269-274.

Costa M, Brookes SJ, Steele PA, Gibbins I, Burcher E and Kandiah CJ (1996) Neurochemical classification of myenteric neurons in the guinea-pig ileum. *Neuroscience* **75**(3):949-967.

Ducic I, Caruncho HJ, Zhu WJ, Vicini S and Costa E (1995) gamma-Aminobutyric acid gating of Cl- channels in recombinant GABAA receptors. *J Pharmacol Exp Ther* **272**(1):438-445.

Ebert B, Wafford KA, Whiting PJ, Krogsgaard-Larsen P and Kemp JA (1994) Molecular pharmacology of gamma-aminobutyric acid type A receptor agonists and partial agonists in oocytes injected with different alpha, beta, and gamma receptor subunit combinations. *Mol Pharmacol* **46**(5):957-963.

Enna SJ (2012) The GABA Receptors, in *The Receptors* (Enna SJ and Mohler H eds), Humana Press Inc., Totowa, NJ.

Farrar SJ, Whiting PJ, Bonnert TP and McKernan RM (1999) Stoichiometry of a ligand-gated ion channel determined by fluorescence energy transfer. *J Biol Chem* **274**(15):10100-10104.

Fletcher EL, Clark MJ, Senior P and Furness JB (2001) Gene expression and localization of GABA(C) receptors in neurons of the rat gastrointestinal tract. *Neuroscience* **107**(1):181-189.

Frisch GWTMJ, Schlegel HB, Scuseria GE, Robb MA, Cheeseman JR, Montgomery JA, Vreven T, Kudin KN, Burant JC, Millam JM, Iyengar SS, Tomasi J, Barone V, Mennucci B, Cossi M, Scalmani G, Rega N, Petersson GA, Nakatsuji H, Hada M, Ehara M, Toyota K, Fukuda R, Hasegawa J, Ishida M, Nakajima T, Honda Y, Kitao O, Nakai H, Klene M, Li X, Knox JE, Hratchian HP, Cross JB, Bakken V, Adamo C, Jaramillo J, Gomperts R, Stratmann RE, Yazyev O, Austin AJ, Cammi R, Pomelli C, Ochterski JW, Ayala PY, Morokuma K, Voth GA, Salvador P, Dannenberg JJ, Zakrzewski VG, Dapprich S, Daniels AD, Strain MC, Farkas O, Malick DK, Rabuck AD, Raghavachari K, Foresman JB, Ortiz JV, Cui Q, Baboul AG, Clifford S, Cioslowski J, Stefanov BB, Liu G, Liashenko A, Piskorz P, Komaromi I, Martin RL, Fox DJ, Keith T, Al-Laham MA, Peng CY, Nanayakkara A, Challacombe M, Gill PMW, Johnson B, Chen W, Wong MW, Gonzalez C and Pople JA (2004), Gaussian v03, Gaussian, Inc., Wallingford CT.

Furness JB, Kunze WA, Bertrand PP, Clerc N and Bornstein JC (1998) Intrinsic primary afferent neurons of the intestine. *Prog Neurobiol* **54**(1):1-18.

Galligan JJ (2002) Ligand-gated ion channels in the enteric nervous system. *Neurogastroenterol Motil* **14**(6):611-623.

Giannotti D, Viti G, Nannicini R, Pestellini V and Bellarosa D (1995) *Bioorg Med Chem Lett* **5**(14):1461-1466.

Giannotti D, Viti G, Sbraci P, Pestellini V, Volterra G, Borsini F, Lecci A, Meli A, Dapporto P and Paoli P (1991) New dibenzothiadiazepine derivatives with antidepressant activities. *J Med Chem* **34**(4):1356-1362.

Goldberg, I. (1906) Berichte der deutschen chemischen Gesellschaft. *Ber. Dtsch. Chem. Ges.* **39**(2):1691-1692.

Hadingham KL, Wingrove PB, Wafford KA, Bain C, Kemp JA, Palmer KJ, Wilson AW, Wilcox AS, Sikela JM, Ragan CI and et al. (1993) Role of the beta subunit in determining the pharmacology of human gamma-aminobutyric acid type A receptors. *Mol Pharmacol* **44**(6):1211-1218.

Hanley JG, Koulen P, Bedford F, Gordon-Weeks PR and Moss SJ (1999) The protein MAP-1B links GABA(C) receptors to the cytoskeleton at retinal synapses. *Nature* **397**(6714):66-69.

Harty RF, Boharski MG, Bochna GS, Carr TA, Eagan PE, Rings M, Lassiter DC, Pour MP, Schafer DF and Markin RS (1991) gamma-Aminobutyric acid localization and function as modulator of cholinergic neurotransmission in rat antral mucosal/submucosal fragments. *Gastroenterology* **101**(5):1178-1186.

Harty RF and Franklin PA (1983) GABA affects the release of gastrin and somatostatin from rat antral mucosa. *Nature* **303**(5918):623-624.

Jensen ML, Timmermann DB, Johansen TH, Schousboe A, Varming T and Ahring PK (2002) The beta subunit determines the ion selectivity of the GABAA receptor. *J Biol Chem* **277**(44):41438-41447.

Jian HH and Tour JM (2003) En route to surface-bound electric field-driven molecular motors. *J Org Chem* **68**(13):5091-5103.

Karanjia R, Garcia-Hernandez LM, Miranda-Morales M, Somani N, Espinosa-Luna R, Montano LM and Barajas-Lopez C (2006) Cross-inhibitory interactions

between GABAA and P2X channels in myenteric neurones. *Eur J Neurosci* **23**(12):3259-3268.

Kenakin R (1993) Pharmacologic Analysis of Drug–receptor Interaction. *2nd Ed Raven Press, Ltd, New York, NY*.

Kirsch J, Langosch D, Prior P, Littauer UZ, Schmitt B and Betz H (1991) The 93-kDa glycine receptor-associated protein binds to tubulin. *J Biol Chem* **266**(33):22242-22245.

Kneussel M, Brandstatter JH, Laube B, Stahl S, Muller U and Betz H (1999) Loss of postsynaptic GABA(A) receptor clustering in gephyrin-deficient mice. *J Neurosci* **19**(21):9289-9297.

Kofuji P, Wang JB, Moss SJ, Huganir RL and Burt DR (1991) Generation of two forms of the gamma-aminobutyric acidA receptor gamma 2-subunit in mice by alternative splicing. *J Neurochem* **56**(2):713-715.

Krantis A (2000) GABA in the Mammalian Enteric Nervous System. *News Physiol Sci* **15**:284-290.

Krehan D, Storustovu SI, Liljefors T, Ebert B, Nielsen B, Krogsgaard-Larsen P and Frolund B (2006) Potent 4-arylalkyl-substituted 3-isothiazolol GABA(A) competitive/noncompetitive antagonists: synthesis and pharmacology. *J Med Chem* **49**(4):1388-1396.

Krivoshein AV and Hess GP (2006) On the mechanism of alleviation by phenobarbital of the malfunction of an epilepsy-linked GABA(A) receptor. *Biochemistry* **45**(38):11632-11641.

Krystal JH, Sanacora G, Blumberg H, Anand A, Charney DS, Marek G, Epperson CN, Goddard A and Mason GF (2002) Glutamate and GABA systems as targets for novel antidepressant and mood-stabilizing treatments. *Mol Psychiatry* **7 Suppl 1**:S71-80.

Le Novere N, Corringer PJ and Changeux JP (2002) The diversity of subunit composition in nAChRs: evolutionary origins, physiologic and pharmacologic consequences. *J Neurobiol* **53**(4):447-456.

Miranda-Morales M, Garcia-Hernandez LM, Ochoa-Cortes F, Espinosa-Luna R, Naranjo-Rodriguez EB and Barajas-Lopez C (2007) Cross-talking between 5-HT3 and GABAA receptors in cultured myenteric neurons. *Synapse* **61**(9):732-740.

Mohler H (2011) The rise of a new GABA pharmacology. *Neuropharmacology* **60**(7-8):1042-1049.

Nishi S and North RA (1973) Intracellular recording from the myenteric plexus of the guinea-pig ileum. *J Physiol* **231**(3):471-491.

Olsen RW (2006) Picrotoxin-like channel blockers of GABAA receptors. *Proc Natl Acad Sci U S A* **103**(16):6081-6082.

Ortells MO and Lunt GG (1995) Evolutionary history of the ligand-gated ion-channel superfamily of receptors. *Trends Neurosci* **18**(3):121-127.

Poulter MO, Singhal R, Brown LA and Krantis A (1999) GABA(A) receptor subunit messenger RNA expression in the enteric nervous system of the rat: implications for functional diversity of enteric GABA(A) receptors. *Neuroscience* **93**(3):1159-1165.

Saeed A and Rama H (1997) *J Chem Soc Pak* **19**(3):236-239.

Shen KZ and Surprenant A (1993) Somatostatin-mediated inhibitory postsynaptic potential in sympathetically denervated guinea-pig submucosal neurones. *J Physiol* **470**:619-635.

Shou WG, Li JA, Guo TX, Lin ZY and Jia GC (2009) Ruthenium-Catalyzed Intramolecular Amination Reactions of Aryl- and Vinylazides. *Organometallics* **28**(24):6847-6854.

Sieghart W, Ramerstorfer J, Sarto-Jackson I, Varagic Z and Ernst M (2012) A novel GABAA receptor pharmacology: drugs interacting with the a(+) b(-) interface. *Br. J. Pharmacol* **166**:476-485.

Sigel E, Baur R, Trube G, Mohler H and Malherbe P (1990) The effect of subunit composition of rat brain GABAA receptors on channel function. *Neuron* **5**(5):703-711.

Silvestri R, Marfe G, Artico M, La Regina G, Lavecchia A, Novellino E, Morgante E, Di Stefano C, Catalano G, Filomeni G, Abruzzese E, Ciriolo MR, Russo MA, Amadori S, Cirilli R, La Torre F and Sinibaldi Salimei P (2006) Pyrrolo[1,2-b][1,2,5]benzothiadiazepines (PBTDs): A new class of agents with high apoptotic activity in chronic myelogenous leukemia K562 cells and in cells from patients at onset and who were imatinib-resistant. *J Med Chem* **49**(19):5840-5844.

Sokolova E, Nistri A and Giniatullin R (2001) Negative cross talk between anionic GABAA and cationic P2X ionotropic receptors of rat dorsal root ganglion neurons. *J Neurosci* **21**(14):4958-4968.

Stokes BJ, Jovanovic B, Dong HJ, Richert KJ, Riell RD and Driver TG (2009) Rh-2(II)-Catalyzed Synthesis of Carbazoles from Biaryl Azides. *J Org Chem* **74**(8):3225-3228.

Swope SL, Moss SJ, Raymond LA and Huganir RL (1999) Regulation of ligand-gated ion channels by protein phosphorylation. *Adv Second Messenger Phosphoprotein Res* **33**:49-78.

Tsai LH, Tsai W and Wu JY (1993) Action of myenteric GABAergic neurons in the guinea pig stomach. *Neurochem Int* **23**(2):187-193.

Tsao ML, Gritsan N, James TR, Platz MS, Hrovat DA and Borden WT (2003) Study of the chemistry of ortho- and para-biphenylnitrenes by laser flash photolysis and time-resolved IR experiments and by B3LYP and CASPT2 calculations. *J Am Chem Soc* **125**(31):9343-9358.

Twyman RE, Rogers CJ and Macdonald RL (1989) Differential regulation of gamma-aminobutyric acid receptor channels by diazepam and phenobarbital. *Ann Neurol* **25**(3):213-220.

Wang H, Bedford FK, Brandon NJ, Moss SJ and Olsen RW (1999) GABA(A)-receptor-associated protein links GABA(A) receptors and the cytoskeleton. *Nature* **397**(6714):69-72.

Weber A (1966a) 5,5-dioxodibenzo[1, 2, 5]-thiadiazepines and intermediates therefor. U.S. Patent 3268557.

Weber A (1966b) 5,5-dioxodibenzo[1, 2, 5]thiadiazepines derivatives and method of use. U.S. Patent 3274058.

Weber A and Frossard J (1966) [Research on tricyclic psychotropic drugs. Dibenzothiadizepines]. *Ann Pharm Fr* **24**(6):445-450.

Wellendorph P and Brauner-Osborne H (2009) Molecular basis for amino acid sensing by family C G-protein-coupled receptors. *Br J Pharmacol* **156**(6):869-884.

Zhou X and Galligan JJ (2000) GABA(A) receptors on calbindin-immunoreactive myenteric neurons of guinea pig intestine. *J Auton Nerv Syst* **78**(2-3):122-135.

APPENDIX A

Molecules **2013**, *18*, 894-913; doi:10.3390/molecules18010894

OPEN ACCESS

molecules

ISSN 1420-3049

www.mdpi.com/journal/molecules

Article

Dibenzo[1,2,5]thiadiazepines Are Non-Competitive $GABA_A$ Receptor Antagonists

Juan F. Ramírez-Martínez [1,2], Rodolfo González-Chávez [2], Raquel Guerrero-Alba [1], Paul E. Reyes-Gutiérrez [2], Roberto Martínez [3], Marcela Miranda-Morales [4], Rosa Espinosa-Luna [1], Marco M. González-Chávez [2,*] and Carlos Barajas-López [1,*]

[1] División de Biología Molecular, Instituto Potosino de Investigación Científica y Tecnológica, San Luis Potosí 78216, Mexico; E-Mails: francisco.martinez@uaslp.mx (J.F.R.-M.); biogigio@hotmail.com (R.G.-A.); respinosa@ipicyt.edu.mx (R.E.-L.)

[2] Facultad de Ciencias Químicas, Universidad Autónoma de San Luis Potosí, San Luis Potosí 78210, Mexico; E-Mails: rodolfo.gonzalez@uaslp.mx (R.G.-C.); pa_edu3@yahoo.com.mx (P.E.R.-G.)

[3] Instituto de Química, Universidad Nacional Autónoma de México, Coyoacán 04510, Mexico; E-Mail: robmar@servidor.unam.mx

[4] Departamento de Neurobiología Celular y Molecular, Instituto de Neurobiología, Universidad Nacional Autónoma de México, Querétaro 76230, Mexico; E-Mail: mmirandam@unam.mx

* Authors to whom correspondence should be addressed; E-Mails: gcmm@uaslp.mx (M.M.G.-C.); cbarajas@ipicyt.edu.mx (C.B.-L.); Tel.: +52-444-826-2440 (ext. 526) (M.M.G.-C.); Tel.: +52-444-834-2035 (C.B.-L.); Fax: +52-444-834-2010 (C.B.-L.).

Received: 14 December 2012; in revised form: 31 December 2012 / Accepted: 5 January 2013 / Published: 11 January 2013

Abstract: A new process for obtaining dibenzo[c,f][1,2,5]thiadiazepines (DBTDs) and their effects on $GABA_A$ receptors of guinea pig myenteric neurons are described. Synthesis of DBTD derivatives began with two commercial aromatic compounds. An azide group was obtained after two sequential reactions, and the central ring was closed via a nitrene to obtain the tricyclic sulfonamides (DBTDs). Whole-cell recordings showed that DBTDs application did not affect the holding current but inhibited the currents induced by GABA (I_{GABA}), which are mediated by $GABA_A$ receptors. These DBTDs effects reached their maximum 3 min after application and were: (i) reversible, (ii) concentration-dependent (with a rank order of potency of **2c** = **2d** > **2b**), (iii) mediated by a non-competitive antagonism, and (iv) only observed when applied extracellularly. Picrotoxin (which binds in the channel mouth) and DBTDs effects were not modified when both substances were

simultaneous applied. Our results indicate that DBTD acted on the extracellular domain of $GABA_A$ channels but independent of the picrotoxin, benzodiazepine, and GABA binding sites. DBTDs used here could be the initial model for synthesizing new $GABA_A$ receptor inhibitors with a potential to be used as antidotes for positive modulators of these receptors or to induce experimental epilepsy.

Keywords: dibenzothiadiazepines; $GABA_A$ receptor antagonists; patch clamp; neurochemistry; biological activity; enteric neurons; electrophysiology

1. Introduction

The synthesis of tricyclic compounds with a central thiadiazepine ring (see Figure 1, **1** ring B) were first described by Weber [1], followed by a description of the compounds anti-depressive effects (compound **1a**) [2,3]. In 1991, Giannotti *et al.* [4] prepared DBTD (compound **1b**) structural variants at nitrogen 11 (N-11) with the purpose of increasing the antidepressive effects previously observed by Weber, while reducing possible side effects. In addition to the effects of DBTDs on the central nervous system, these substances were found to act as non-nucleosidic reverse transcriptase inhibitors of HIV-1 (compound **1c**) [5] and to have anti-proliferative activity on leukemia cell lines (compound **1d**) [6], effects that increased the attention toward these tricyclic compounds.

Figure 1. General chemical structure of the dibenzo[*c,f*][1,2,5]thiadiazepines **1**, and several DBTDs reported to have biological activity (compounds **1a**, **1b**, **1c**, and **1d**).

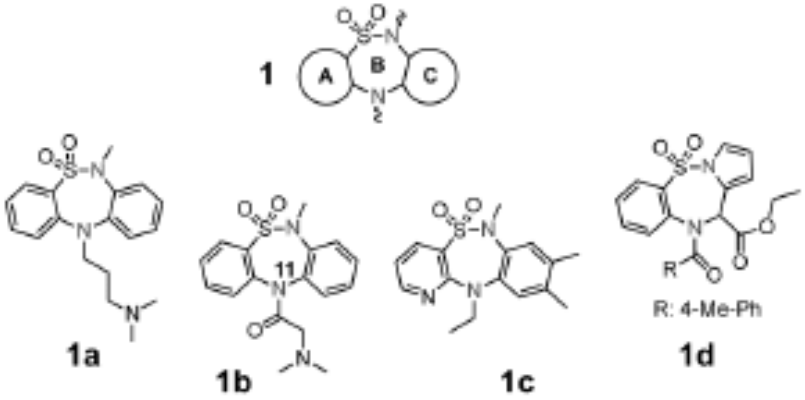

The central ring of DBTDs has been synthesized via the Goldberg method, which involves an Ullmann intra-molecular condensation reaction (N-C) (Figure 2, route a) [7]. This reaction is limited by the fact that *ortho*-haloanilines significantly reduce the number of possible substituents that may be included in the DBTDs. Only one report has described the use of this methodology for obtaining compounds **2a** and **2d** [8]. As an alternative approach, N-C bonds may be formed via intra-molecular reactions of aryl azides with benzene derivatives (Figure 2, route b), which has been described during the formation of carbazoles through thermolysis [9], photolysis [10], and recently, via metal

catalysis [11,12]. The advantage of using aryl azides is that C-N bonds are formed directly. Therefore, the use of monosubstituted anilines with diverse functional groups can lead us toward obtaining DBTDs with functional variations in the C ring. Known DBTDs and triheterocyclic analogous compounds include diverse substituents on the nitrogen of the thiadiazepine ring (Figure 1); however, no studies have examined the biological activities of the parent compound and 9-substituted derivatives (Figure 2).

Figure 2. Retrosynthetic analysis of the non-substituted DBTDs. (**a**) Classical method for obtaining 2 by the Goldberg methodology; (**b**) Obtaining 2 from an aryl azide.

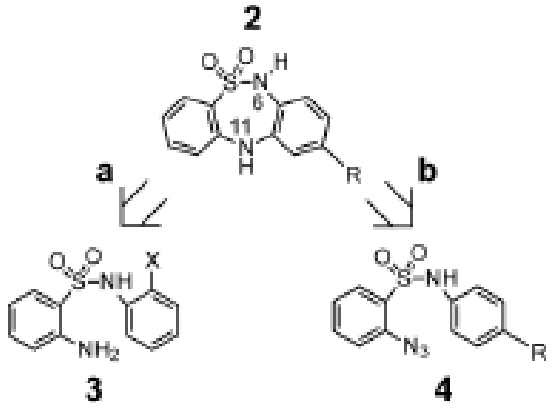

This work is the first report to consider a biological study of DBTDs without substituents on nitrogens 6 and 11 of B ring, which were obtained through a process distinct from the Ullmann method. The presence of a hydrogen atom at N-6 and N-11 in a DBTD can determine the compound's affinity toward proteins via hydrogen bond interactions [13], as shown in Figure 3.

Figure 3. The dotted lines in DBTDs indicate probable interactions between hydrogen bonds and proteins.

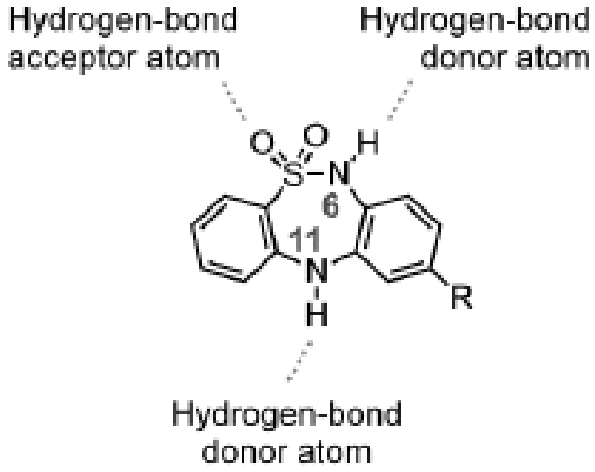

The linear synthetic route to the DBTDs **2a–g** comprises four stages and proceeds as described in Scheme 1. The thiadiazepine ring is formed through direct amination of the C ring via intramolecular thermal cyclization of **4** (Figure 2, route b). This methodology provides an alternative to the classical amination of Goldberg approach, with respect to the formation of ring B in the substituted DBTDs (Figure 2, route a) [2,4,5,8,14]. DBTDs with a modified B ring were shown to have biological effects. Giannotti *et al.* synthesized a series of DBTDs with substituents in the thiadiazepine ring, and they showed that the compounds displayed a potential antidepressive effect using the apomorphine-induced hypothermia test [4]. However, these authors found no binding of DBTDs with receptors to dopamine, serotonin, histamine, benzodiazepine, GABA, acetylcholine, and adrenaline, and reported that DBTDs lack of effect on serotonin and noradrenaline uptake. However, such observations does not rule out that DBTDs might be modulating any of these receptor proteins through a different binding site than the one directly activated by a given agonist or modulator. At least three observations indicated us that $GABA_A$ channels might be the target for DBTDs: (i) the tricyclic sulfonamide **2** is structurally similar to the 1,4-benzodiazepines, which are major positive modulators of these channels [15]; (ii) DBTDs have antidepressive actions [4] and (iii) $GABA_A$ channels have been implicated in mood disorders, including depression [16,17]. Therefore, the aim of the present study was to further investigate the effects of DBTDs on $GABA_A$ channels and to report a new synthetic platform for obtaining DBTD compounds that do not include the thiadiazepine ring substitutions. We found that these compounds inhibit directly $GABA_A$ channels by a mechanism that is independent of the binding sites for GABA, picrotoxin, and benzodiazepine.

Scheme 1. *Reagents and conditions*: (**a**) Anhydrous pyridine, dry acetone, $N_{2(g)}$, 24 h; (**b**) $SnCl_2{\cdot}2H_2O$, ethyl acetate, 4 h; (**c**) first step: $NaNO_2$, F_3CCO_2H, 1 h; second step: NaN_3, 1 h; (**d**) $(C_6H_5)_2O$, 208 °C, 5 min. Compound **2g** was obtained from **2f**: first step: KOH 10%, 1 h.

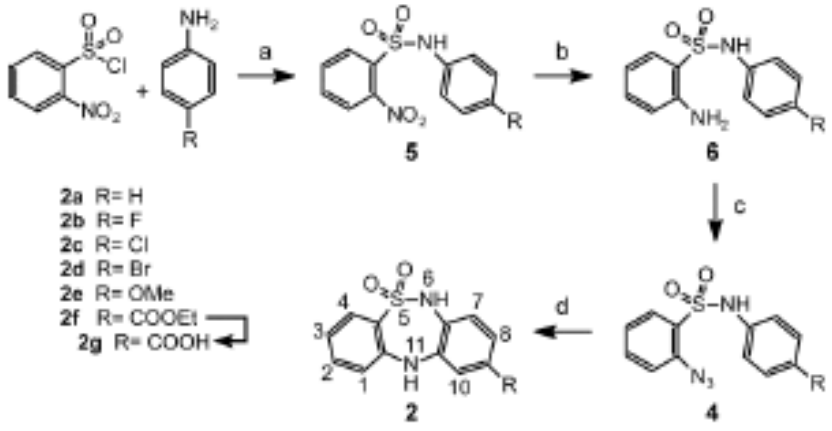

2. Results and Discussion

2.1. Chemistry

The synthetic route begins with the reaction of 4-substituted-anilines with 2-nitrobenzenesulfonyl chloride under reflux using pyridine as the base and acetone as solvent. The 2-nitrosulfonamides **5a–f**

were obtained in good yields (66%–88%). The subsequent catalytic hydrogenation of the nitro group using tin(II) chloride under reflux with ethyl acetate yielded the amines **6a–f** in yields above 88%. The amino compounds were transformed to the corresponding 2-azidobenzensulfonamides through their diazotization with sodium nitrite in trifluoroacetic acid (note that the transformation of **6e** was accomplished using hydrochloric acid). The *in situ* substitution of the diazo group with sodium azide induced conversion to **4a–f** with a 78%–87% yield. In the final step, the thiadiazepine formation reaction proceeded via thermolysis above 208 °C in diphenyl ether, this temperature favoured the formation of an intermediate nitrene reagent [9]. A direct N-C-type amination of the C ring provided the DBTDs **2a–f** with yields of 67%–85%, except for compound **2f**, which was isolated in a yield of 12%. Compound **2g** was obtained by basic hydrolysis of **2f** after a hydrochloric acid treatment.

2.2. Biological Results

The inhibitory effects of DBTDs on the native $GABA_A$ receptors of guinea pig myenteric neurons were studied here for the first time. The Cl^- concentrations outside and inside the neurons were similar, and a holding potential was −60 mV. At this potential, GABA (0.03–3 mM) induced inward currents (I_{GABA}) in 86% of myenteric neurons. The amplitude of the currents was concentration-dependent (EC_{50} = 115 ± 10 μM) and varied among the different neurons with a range of 0.1–6 nA, in response to 300 μM GABA. Most neurons maintained a stable value of I_{GABA} during repeated GABA applications. Otherwise, the data were rejected. In order to test that these GABA currents are mediated by $GABA_A$ channels bicuculline (0.1–100 μM) and picrotoxin (3–1,000 μM) were used, inhibitors of these receptors [18–20]. Both substances inhibited I_{GABA} in a concentration-dependent manner (data not shown) with an IC_{50} of 10 ± 2 and 6 ± 1 μM, respectively. Maximal concentrations used for both antagonists virtually abolished I_{GABA}, as it was previously reported [18–20].

Figure 4 shows that application of DBTDs (100 μM) inhibited the currents induced by GABA (300 μM) in a time-dependent manner (3–180 s) with time constants (t) of 4.9, 2.6, and 29.3 s for **2b**, **2c**, and **2d**, respectively. These constants were calculated by fitting the data using the Michaelis–Menten equation (R^2 = 0.98, 0.88, and 0.99, respectively). The maximum inhibition induced by **2b** and **2c** (100 μM) was reached 3 min after initial exposure. For **2d**, the time required to reach the maximum inhibition was calculated to be 17 min; however, the experimental maximum inhibition observed after a 3 min treatment was 74.2 ± 2.4% (n = 10), similar to the calculated maximum inhibition (87.0 ± 3.0%). In all subsequent experiments, a DBTD treatment time of 3 min was used. The current inhibition induced by **2b**, **2c**, and **2d** was fully reversed within five minutes of washing. The holding current remained constant in the presence of the compounds at all concentrations tested, indicating that the compounds could not open the $GABA_A$ receptors or any other neuronal ion channel under the experimental conditions.

Control experiments were conducted using DMSO, the solvent used for all DBTDs, demonstrating that DMSO did not modify the properties of I_{GABA} alone at the maximum concentration used here, 0.33% V/V (data not shown). The inhibitory activities of the DBTDs were likely to be use-independent because their effects did not require active $GABA_A$ receptors and the inhibitory activity increased over time, despite the absence of the agonist (GABA) [21]. This indicates that DBTDs bind to these channels during their closed stage.

Figure 4. Halogenated DBTDs inhibited the I_{GABA} in a time-depended manner. (**A**) I_{GABA} was recorded before, during application of 100 μM **2b**, and after removal of the inhibitor of a given myenteric neuron for various lengths of time. The horizontal bars above the traces indicate the application profiles of the indicated substances. (**B**) Time course of I_{GABA} (induced by 300 μM GABA) inhibition induced by **2** over 3–180 s. Michaelis–Menten fits. Each data point represents the mean value from 3–12 different experiments. The lines represent the SEM.

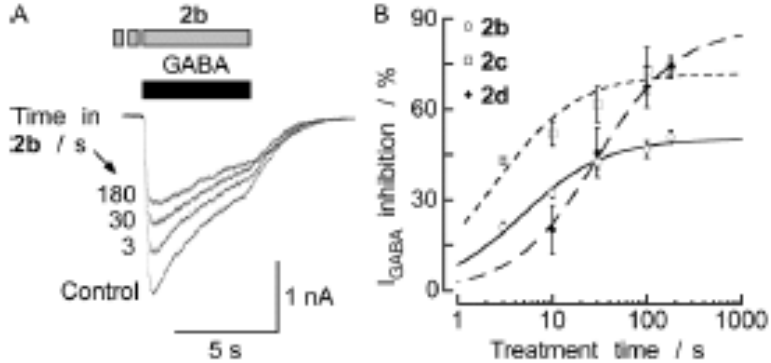

The inhibitory effects of seven DBTDs at a 100 μM concentration are listed in Table 1. The data indicate that the rank order of potency for these inhibitors was **2c** = **2d** > **2b**; we were unable to calculate the potency of **2f**, **2e**, **2a**, **2g** due to solubility problems. Figure 5 shows the concentration–response curves for the inhibitory effects of three DBTDs (3–1,000 μM) on the currents induced by GABA (300 μM). The maximum effect of **2b** was achieved at 1 mM (inducing a complete inhibition of the GABA-activated currents), and an IC_{50} value (104 ± 9.2 μM). We did not reach the maximum inhibition for **2c** and **2d** because the compounds were insoluble at concentrations exceeding 300 μM under our experimental conditions. Curve fits were obtained in both cases with IC_{50} values of 50.4 ± 6.4 μM and 47.6 ± 30.3 μM for **2c** and **2d**, respectively.

Table 1. Percent inhibition in the presence of 100 μM compounds on GABA-induced inward currents, p IC_{50}, cLog *P*, and physical data.

No.	Percentage of inhibition [a]	p IC_{50}/M	cLog *P* [b]	Yield/%	mp/°C
2a	28.4 ± 1.4 (5)	ND	2.18	69	198
2b	50.8 ± 2.1 (12)	3.98	1.50	70	202
2c	74.2 ± 3.6 (6)	4.30	2.69	79	248
2d	74.2 ± 2.4 (10)	4.32	2.97	85	250
2e	43.7 ± 3.8 (3)	ND	1.92	67	171
2f	47.1 ± 3.7 (7)	ND	2.25	12	227
2g	16.0 ± 2.4 (6)	ND	1.87	100	350

[a] Values are given as the mean ± SEM, with the number of experiments in parentheses; [b] Data generated using HyperChem.

Figure 5. DBTDs inhibited I_{GABA} in a concentration-dependent manner. (**A**) Representative I_{GABA} recordings from a myenteric neuron in the presence of various concentrations of **2b**, which was added 3 min before GABA application. (**B**) Concentration—response curves for the effects of the DBTDs on the amplitude of I_{GABA}. The lines indicate fits to the experimental data using a two-parameter logistic function, [22] assuming an inhibition of 100%. Each data point represents the mean ± SEM from 3–12 individual experiments.

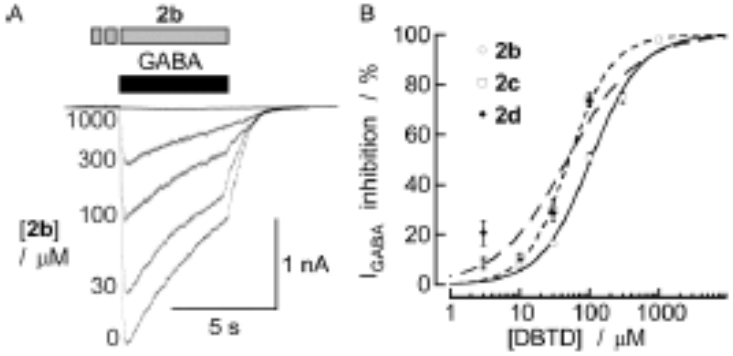

We considered the possibility that because these novel substances were highly lipophilic (log *P* ~ 2.0 for all compounds, Table 1), the DBTDs could permeate the neuron membrane and interact with the inner part of the $GABA_A$ channel, thereby inhibiting I_{GABA}. To investigate this possibility, we added 100 μM **2b** to the pipette solution (internal) and monitored I_{GABA}, and we applied **2b** to the outside of the cells and monitored the inhibitory effects (Figure 6). Experiments were performed using **2b**, even though cLog *P* was less than 2, because **2c** and **2d** were insoluble under the conditions employed. The amplitude of I_{GABA} (300 μM) for neurons with **2b** (100 μM) applied inside (−1408 ± 344 pA; n = 4) and measured 2 to 3 min after obtaining the whole cell configuration did not differ from the amplitude of the control I_{GABA} (−1510 ± 333 pA; n = 12) of experiments in which **2b** was tested extracellularly. Consistent with these findings, in recordings with **2b** in the pipette, the amplitude of I_{GABA} was the same 5 min (−1536 ± 379 pA) and 10 min (−1604 ± 409 pA; n = 4) after obtaining the whole-cell configuration. In addition, the presence of **2b** inside the neurons did not affect the magnitude of the inhibition induced by the extracellular application of **2b** (100 μM). Thus, such an inhibition was as large as that observed without **2b** inside the cells (Figure 6B). Altogether, these data rule out that DBTDs inhibitory effects on $GABA_A$ channels are mediated by an intracellular target and therefore, they must be acting on the extracellular domain.

Figure 7 shows two concentration-response curves for the effects of GABA, one in the absence and the other in the presence of 100 μM **2b**. As shown, the antagonistic effect of **2b** is not surmounted by increasing the GABA concentration. Indeed, the EC_{50} values for these curves were 127 ± 16 and 123 ± 84 μM in the absence and in the presence of **2b**, whereas, the maximum inhibition clearly decreased in the presence of **2b** (~50%) across the full GABA concentration–response curve. Our data demonstrate that the pharmacological antagonism by which **2b** inhibits the $GABA_A$ receptors is non-competitive and therefore, it is unlikely acting at the GABA binding site. This is in agreement with a previous study [4] that shows no binding of DBTDs to GABA receptors.

Figure 6. The inhibitory effects of **2b** on $GABA_A$ receptors were mediated by an extracellular binding site. A) I_{GABA} for a 100 μM concentration of **2b** in the pipette (**2b**$_{-/i}$), 10 min after obtaining the whole cell. I_{GABA} was recorded before (-/i) and in presence of extracellular (o/i) **2b** (100 μM for 3 min). B) Bars indicate the average amplitude of I_{GABA}, and the lines above indicate the SEM. I_{GABA} amplitude or the inhibitory effect of **2b** did not differ significantly (NS) by the presence of **2b** inside the pipette. Statistical comparison of the data was done using the unpaired Student's *t*-test.

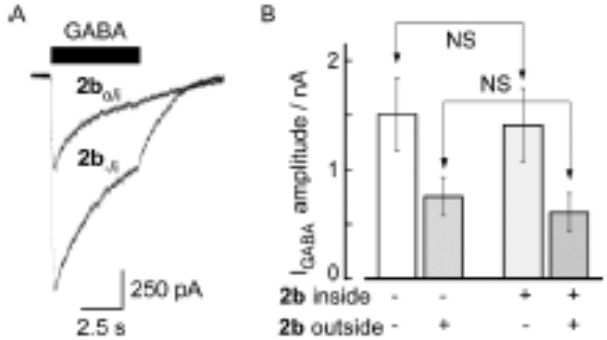

Figure 7. **2b** inhibits I_{GABA} in a non-competitive manner. (**A**) Concentration–response curves for GABA in the absence (Control) and in the presence of **2b**. Responses were normalized with respect to the curves obtained in the presence of 3 mM GABA in each cell and in the absence of **2b**. Each point represents the mean ± SEM for 5–12 neurons. The lines indicate fits of experimental data to a three-parameter logistic function.

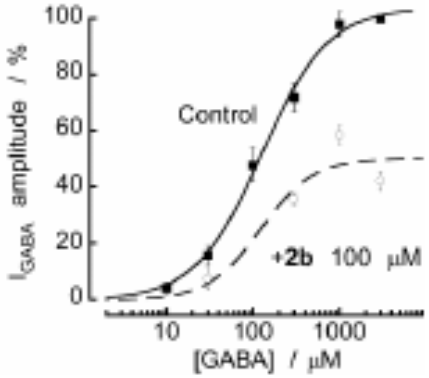

We further investigated if the inhibitory effect of DBTD on I_{GABA} was voltage dependent by conducting experiments at two holding membrane potentials, −60 mV and +40 mV in the same neurons. I_{GABA} (300 μM) was recorded in the absence or presence of 100 μM **2b**, **2c**, and **2d**. As shown in Figure 8, the inhibitory effects induced by any of the three substances were identical for an inward I_{GABA} (recorded at −60 mV) than for the outward I_{GABA} (recorded at +40 mV). These results indicate that the DBTDs inhibit I_{GABA} via a voltage-independent mechanism.

Figure 8. The inhibitory effects of compounds 2 on $GABA_A$ channels were voltage independent. A) I_{GABA} induced by 300 μM GABA without (Control) or in presence of **2c** (100 μM) at −60 mV (upper traces) and +40 mV (lower traces) from the same neuron. I_{GABA} was recorded at 5 min intervals, and **2c** was applied 3 min before the second GABA application. B) The average (bars) inhibitory effect of **2b**, **2c**, and **2d** was the same at both membrane potentials. Lines over the bars indicate the SEM.

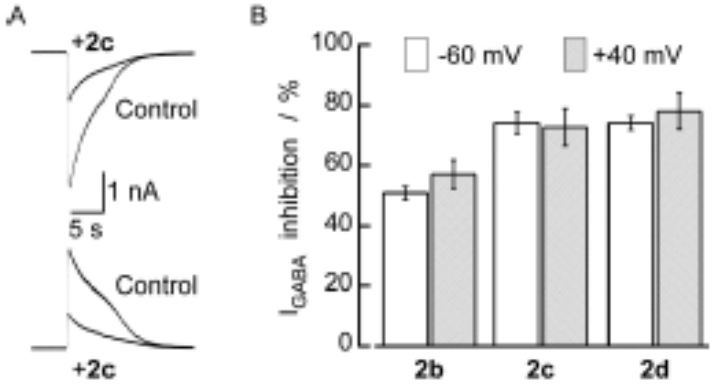

The fact that binding of compounds 2 on $GABA_A$ channels can occur during the close stage and is voltage-independent suggests that its binding site is not within the channel pore. In order to further investigate this, we tested if picrotoxin interacts with the binding of **2c**. Picrotoxin is known to bind into a site within the channel formed by the second transmembrane domains of the five subunits constituting the $GABA_A$ receptors [23,24]. We found that neither picrotoxin effect was modified by **2c** nor the inhibitory effect of **2c** was affected by picrotoxin (Figure 9), which would indicate that **2c** does not bind into the picrotoxin binding site.

Figure 9. **2c**-induced inhibition of $GABA_A$ channels was unaffected by picrotoxin (PTx). Bars and lines on their top, are means and SEM (n = 4). Statistical comparison of each pair of bars was done using the paired Student's *t*-test. P values and non significant (NS) differences are indicated.

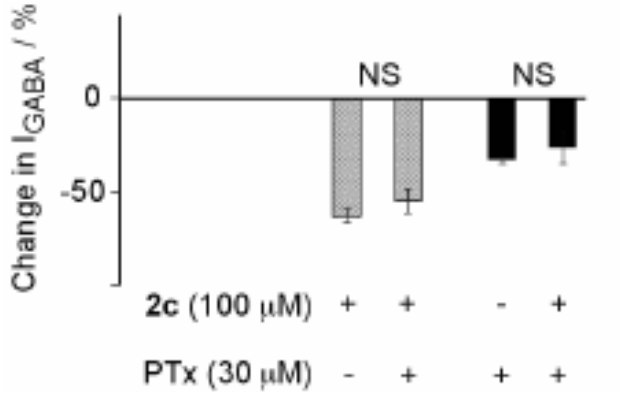

The tricyclic sulfonamide **2** is also structurally similar to the 1,4-benzodiazepines, hence, the inhibitory actions of DBTDs may be related to the benzodiazepine modulator sites. The inhibitory effects of **2b**, **2c**, and **2d** remained constant in the absence and presence of flumazenil, a known antagonist of the benzodiazepine site on the $GABA_A$ receptors (Figure 10). Inhibition by 100 μM **2b**, **2c**, and **2d** without flumazenil (50.8 ± 2.1%, 74.2 ± 3.6%, 74.2 ± 2.4%, respectively) was not blocked by the co-application of 10 μM flumazenil (47.8 ± 5.8%, 69.6 ± 5.2%, 68.4 ± 6.8%, respectively). The same concentration of flumazenil, applied for 3 min, did not induce changes in the holding current or I_{GABA} in experiments carried out using five different neurons (data not shown). We showed that **2b** did not act through the benzodiazepine binding site, which is in agreement with the lack of binding with receptors to benzodiazepine, previously reported [4].

Figure 10. The inhibitory effects of compounds **2** on the $GABA_A$ channels were independent of the benzodiazepine binding site. (**A**) First and last traces represent control currents induced by GABA (300 μM). The two middle traces were recorded in **2d** (100 μM) alone or plus flumazenil (10 μM), all traces are from the same neuron. (**B**) Each pair of bars represents the mean inhibition of I_{GABA} induced by DBTDs, before (Control) and in the presence of flumazenil. Lines over the bars indicate the SEM.

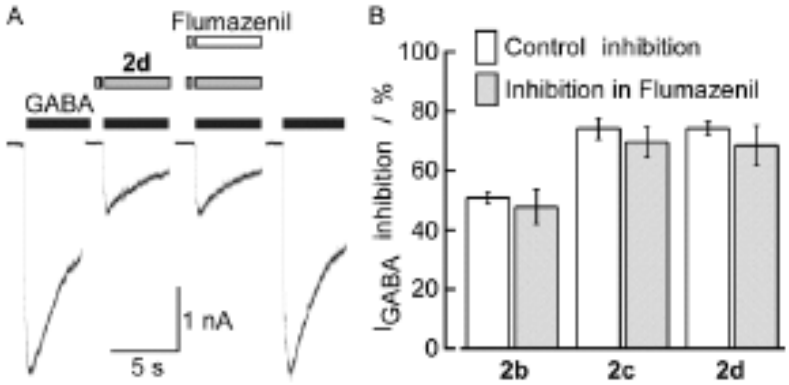

3. Experimental

3.1. Chemistry

3.1.1. General

All reagents and solvents were reagent-grade and were used as received from Sigma-Aldrich Co. (St. Louis, MO, USA). Flash chromatography was performed using Merk Kiesegel 60 silica gel (230–400 mesh). Melting points are reported uncorrected. The FTIR spectra were recorded on a Thermo Nicolet Nexus 470 FTIR as thin films on a KBr disk (for solids) or a germanium ATR crystal (for liquids). ^{1}H-NMR and ^{13}C-NMR spectra were obtained using an Eclipse Jeol (operating at 300 and 75 MHz, respectively) and a Varian-Gemini (operated at 200 MHz and 50 MHz, respectively), and the signals are reported in ppm relative to TMS. All mass spectra (MS) were recorded on a Jeol AX505HA mass spectrometer. Elemental analyses were performed on a CE-440 Exeter Analytical Inc.

3.1.2. General Procedures for Synthesizing *N*-(4-(*R*)-Phenyl)-2-nitrobenzenesulfonamides **5a–f**

Anhydrous pyridine (1.10 mL, 13.6 mmol) and 4-*R*-aniline (1.24 mL, 13.6 mmol) in dry acetone were added, via cannula, to a stirred solution of 2-nitrobenzenesulfonyl chloride (3.01 g, 13.6 mmol) in dry acetone (25 mL) under nitrogen, and the reaction mixture was stirred at room temperature. After 24 h the mixture was neutralized with a saturated sodium bicarbonate solution, and the resulting solid was collected, washed with water and ethanol, and dried under vacuum. The solid was purified by flash chromatography (silica gel, eluting with 90:10 hexane–ethyl acetate), then recrystallized from ethyl acetate–hexane (30:70) to obtain **5a** as a white solid (11.97 mmol, 88%); m.p.: 118–119 °C. The same procedure was used for the synthesis of **5b–5f**. Products **5**, **6**, and **4** (except for series **f**) were first reported by Saeed and Rama [25]. However, **5** and **6** compounds were not characterized and **4** was only partially characterized by IR and MS spectroscopies.

N-(Phenyl)-2-nitrobenzenesulfonamide (**5a**). ^{1}H-NMR (300 MHz, $CDCl_3$ + DMSO-d_6): δ = 7.08 (m, 1H), 7.21 (m, 4H), 7.63 (ddd, J_o = 7.5 Hz, J_m = 1.6 Hz, 1H), 7.70 (ddd, J_o = 7.5 Hz, J_m = 1.6 Hz, 1H), 7.76 (dd, J_o = 8.0 Hz, J_m = 1.6 Hz, 1H), 7.92 (dd, J_o = 7.9 Hz, J_m = 1.6 Hz, 1H), 9.9 ppm (s, 1H); IR (KBr): ν = 3324, 1380, 1180 cm^{-1}; MS (EI, 70 eV): *m/z*: 278 [M]$^+$.

N-(4-Fluorophenyl)-2-nitrobenzenesulfonamide (**5b**). Yellow crystals. Yield 79%; m.p.: 106 °C; ^{1}H-NMR (200 MHz, DMSO-d_6): δ = 7.13 (d, J_o = 6.8 Hz, 4H), 7.88 (m, 4H), 10.7 ppm (s, 1H); IR (KBr): ν = 3293, 1360, 1160 cm^{-1}; MS (EI, 70 eV): *m/z*: 296 [M]$^+$.

N-(4-Chlorophenyl)-2-nitrobenzenesulfonamide (**5c**). Yellow crystals. Yield 66%; m.p.: 122 °C; ^{1}H-NMR (200 MHz, DMSO-d_6): δ = 7.13 (d, J_o = 9.0 Hz, 2H), 7.35 (d, J_o = 9.0 Hz, 2H), 7.89 (m, 4H), 10.9 ppm (s, 1H); IR (KBr): ν = 3309, 1334, 1162 cm^{-1}; MS (EI, 70 eV): *m/z*: 312 [M]$^+$.

N-(4-Bromophenyl)-2-nitrobenzenesulfonamide (**5d**). Colorless crystals. Yield 79%; m.p.: 118 °C; ^{1}H-NMR (200 MHz, DMSO-d_6): δ = 7.06 (d, J_o = 9.0 Hz, 2H), 7.47 (d, J_o = 8.8 Hz, 2H), 7.91 (m, 4H), 10.9 ppm (s, 1H); IR (KBr): ν = 3297, 1363, 1164 cm^{-1}. MS (EI, 70 eV): *m/z*: 358/356 [M]$^+$.
N-(4-Methoxyphenyl)-2-nitrobenzenesulfonamide (**5e**). Yellow needle crystals. Yield 72%; m.p.: 90 °C; ^{1}H-NMR (200 MHz, DMSO-d_6): δ = 3.67 (s, 3H), 6.83 (d, J_o = 9.0 Hz, 2H), 7.03 (d, J_o = 9.0 Hz, 2H), 7.87 (m, 4H), 10.4 ppm (s, 1H); IR (KBr): ν = 3259, 1361, 1172 cm^{-1}; MS (EI, 70 eV): *m/z*: 308 [M]$^+$.

Ethyl-4-(2-nitrophenylsulfonamido)benzoate (**5f**). Brown solid. Yield 82%; m.p.: 172 °C; ^{1}H-NMR (300 MHz, DMSO-d_6): δ = 1.25 (t, J_o = 7.1 Hz, 3H), 4.22 (q, J_o = 7.1 Hz, 2H), 7.13 (BB', J_o = 8.7 Hz, 2H), 7.75 (ddd, J_o = 7.5 Hz, 1H), 7.78 (AA', J_o = 8.7 Hz, 2H), 7.79 (ddd, J_o = 7.5 Hz, 1H), 7.91 (dd, J_o = 6.6 Hz, 1H), 7.98 ppm (dd, J_o = 7.0 Hz, 1H); IR (KBr): ν = 3200, 1690, 1365, 1162 cm^{-1}; MS (EI, 70 eV): *m/z*: 350 [M]$^+$.

3.1.3. General Procedures for the Synthesis of 2-Amino-*N*-(4-(*R*) phenyl)benzenesulfonamides **6a–f**

N-(4-(*R*) phenyl)-2-nitrobenzenesulfonamide **5** (4.3 g, 15.6 mmol) and tin (II) chloride dehydrate (14.82 g, 65.7 mmol) were heated in ethyl acetate under reflux for 4 h. The mixture was stirred, and a saturated sodium bicarbonate solution was added to a pH of 6. The solution was extracted with ethyl

acetate. The solvent was removed, and the residue was purified by flash chromatography (eluting with a 90:10 solution of hexane–ethyl acetate).

2-Amino-N-phenylbenzenesulfonamide (**6a**). Yellow powder (14.04 mmol, 90%); m.p.: 123–124 °C; ^{1}H-NMR (300 MHz, DMSO-d_6): δ = 5.99 (s, 2H), 6.54 (ddd, J_o = 7.6 Hz, J_m = 1.2 Hz, 1H), 6.75 (dd, J_o = 8.1 Hz, J_m = 0.9 Hz, 1H), 6.97 (ddd, J_o = 8.2 Hz, 1H), 7.04 (dd, J_o = 8.6 Hz, 2H), 7.2 (m, 3H), 7.49 (dd, J_o = 8.5 Hz, J_m = 1.4 Hz, 1H), 10.2 ppm (s, 1H); IR (KBr): ν = 3457, 3368, 3240, 1360, 1180 cm^{-1}; MS (EI, 70 eV): *m/z*: 248 [M]$^+$.

2-Amino-N-(4-fluorophenyl) benzenesulfonamide (**6b**). Brown liquid. Yield 99%; ^{1}H-NMR (200 MHz, DMSO-d_6): δ = 5.98 (s, 2H), 6.53 (ddd, J_o = 7.05 Hz, J_m = 1.2 Hz, 1H), 6.74 (dd, J_o = 8.3 Hz, J_m = 1.2 Hz, 1H), 7.05 (d, J_o = 6.4 Hz, 4H), 7.21 (ddd, J_o = 7.0 Hz, J_m = 1.6 Hz, 1H), 7.43 (dd, J_o = 8.2 Hz, J_m = 1.6 Hz, 1H), 10.2 ppm (s, 1H); IR (KBr): ν = 3469, 3382, 3284, 1313, 1147 cm^{-1}; MS (EI, 70 eV): *m/z*: 266 [M]$^+$.

2-Amino-N-(4-chlorophenyl) benzenesulfonamide (**6c**). Brown liquid. Yield 99%; ^{1}H-NMR (200 MHz, DMSO-d_6): δ = 6.0 (s, 2H), 6.53 (ddd, J_o = 8.0 Hz, J_m = 1.1, 1H), 6.73 (dd, J_o = 8.3 Hz, J_m = 0.9 Hz, 1H), 7.03 (d, J_o = 8.8 Hz, 2H), 7.2 (ddd, J_o = 8.5 Hz, J_m = 1.6, 1H), 7.26 (d, J_o = 8.8 Hz, 2H), 7.47 (dd, J_o = 8.0 Hz, J_m = 1.6, 1H), 10.4 ppm (s, 1H); IR (KBr): ν = 3467, 3378, 3245, 1313, 1135 cm^{-1}; MS (EI, 70 eV): *m/z*: 282 [M]$^+$.

2-Amino-N-(4-bromophenyl) benzenesulfonamide (**6d**). Brown liquid. Yield 99%; ^{1}H-NMR (200 MHz, DMSO-d_6): δ = 6.0 (s, 2H), 6.55 (ddd, J_o = 7.8 Hz, 1H), 6.76 (dd, J_o = 8.3 Hz, J_m = 0.9 Hz, 1H), 7.0 (d, J_o = 8.8 Hz, 2H), 7.21 (ddd, J_o = 7.0 Hz, J_m = 1.6 Hz, 1H), 7.39 (d, J_o = 8.8 Hz, 2H), 7.49 (dd, J_o = 7.9 Hz, J_m = 1.5 Hz, 1H), 10.4 ppm (s, 1H); IR (KBr): ν = 3482, 3384, 3268, 1319, 1139 cm^{-1}; MS (EI, 70 eV): *m/z*: 328/326 [M]$^+$.

2-Amino-N-(4-methoxyphenyl) benzenesulfonamide (**6e**). Brown liquid. Yield 99%; ^{1}H-NMR (200 MHz, DMSO-d_6): δ = 3.65 (s, 3H), 5.9 (s, 2H), 6.5 (ddd, J_o = 7.7 Hz, J_m = 1.2 Hz, 1H), 6.72 (dd, J_o = 8.7 Hz, 1H), 6.77 (d, J_o = 9.0 Hz, 2H), 6.95 (d, J_o = 9.0 Hz, 2H), 7.19 (ddd, J_o = 8.2 Hz, J_m = 1.6 Hz, 1H), 7.36 (dd, J_o = 8.1 Hz, J_m = 1.6 Hz, 1H), 9.84 ppm (s, 1H); IR (KBr): ν = 3480, 3380, 3266, 1321, 1147 cm^{-1}; MS (EI, 70 eV): *m/z*: 278 [M]$^+$.

Ethyl-4-(2-aminophenylsulfonamido)benzoate (**6f**). Yellow crystals. Yield 88%; m.p.:163 °C; ^{1}H-NMR (200 MHz, DMSO-d_6): δ = 1.25 (t, J_o = 6.3 Hz, 3H), 4.22 (q, J_o = 7.0 Hz, 2H), 6.0 (s, 2H), 6.56 (ddd, J_o = 7.6 Hz, 1H), 6.73 (dd, J_o = 7.8 Hz, 1H), 7.14 (BB', J_o = 8.8 Hz, 2H), 7.22 (ddd, J_o = 7.7 Hz, 1H), 7.57 (dd, J_o = 8.1 Hz, J_m = 1.6 Hz, 1H), 7.79 (AA', J_o = 8.8 Hz, 2H), 10.8 ppm (s, 1H); IR (KBr): ν = 3470, 3380, 3230, 1690, 1322, 1144 cm^{-1}; MS (EI, 70 eV): *m/z*: 320 [M]$^+$.

3.1.4. General Procedures for Synthesizing 2-Azido-*N*-(4-(*R*)phenyl)benzenesulfonamides **4a–f**

An aqueous solution of sodium nitrite (3.6 g, 51.8 mmol) was added to 2-amino-*N*-(4-(*R*)phenyl)benzenesulfonamide **6** (2.86 g, 11.5 mmol) in trifluoroacetic acid, and the reaction mixture was stirred for 1 h. Sodium azide (1.9 g, 28.8 mmol) was added, and the solution was stirred for an

additional 1 h. The mixture was neutralized with saturated sodium bicarbonate solution and extracted with ethyl acetate. The reaction mixture was concentrated and purified by flash chromatography (70:30, hexane–ethyl acetate). The obtained solid was recrystallized in ethyl acetate–hexane (30:70).

2-Azido-N-phenylbenzenesulfonamide (**4a**). Brown powder (9.78 mmol, 85%); m.p.:139 °C; ^{1}H-NMR (200 MHz, DMSO-d_6): d = 6.97 (ddd, J_o = 7.0 Hz, 1H), 7.1 (dd, J_o = 7.4 Hz, 2H), 7.2 (ddd, J_o = 7.4 Hz, 2H), 7.28 (ddd, J_o = 7.6 Hz, 1H), 7.5 (dd, J_o = 8.1 Hz, 1H), 7.64 (ddd, J_o = 7.8 Hz, 1H), 7.86 (dd, J_o = 7.8 Hz, 1H), 10.4 ppm (s, 1H); IR (KBr): ν = 3253, 2133, 1340, 1190 cm^{-1}; MS (EI, 70 eV): *m/z*: 274 [M]$^+$.

2-Azido-N-(4-fluorophenyl) benzenesulfonamide (**4b**). White solid. Yield 83%; m.p.: 129 °C; ^{1}H-NMR (200 MHz, DMSO-d_6): δ = 7.09 (m, 4H), 7.27 (ddd, J_o = 7.3 Hz, J_m = 1.4 Hz, 1H), 7.52 (dd, J_o = 8.0 Hz, J_m = 1.0 Hz, 1H), 7.62 (ddd, J_o = 8.4 Hz, J_m = 1.6 Hz, 1H), 7.8 (dd, J_o = 7.8 Hz, J_m = 1.6 Hz, 1H), 10.2 ppm (s, 1H); IR (KBr): ν = 3249, 2140, 1334, 1166 cm^{-1}; MS (EI, 70 eV): *m/z*: 292 [M]$^+$.

2-Azido-N-(4-chlorophenyl) benzenesulfonamide (**4c**). White crystals. Yield 80%; m.p.: 134 °C; ^{1}H-NMR (200 MHz, DMSO-d_6): δ = 7.11 (d, *Jo* = 8.8 Hz, 2H), 7.27 (d, J_o = 8.8 Hz, 2H), 7.31 (ddd, J_m = 1.1 Hz, 1H), 7.51 (dd, J_o = 8.0 Hz, J_m = 1.4 Hz, 1H), 7.66 (ddd, J_o = 7.7 Hz, J_m = 1.6 Hz, 1H), 7.86 (dd, J_o = 7.8 Hz, J_m = 1.4 Hz, 1H), 10.5 ppm (s, 1H); IR (KBr): ν = 3345, 2132, 1338, 1164 cm^{-1}; MS (EI, 70 eV): *m/z*: 308 [M]$^+$.

2-Azido-N-(4-bromophenyl) benzenesulfonamide (**4d**). Yellow powder. Yield 87%; m.p.: 124 °C; ^{1}H-NMR (200 MHz, DMSO-d_6): δ = 7.05 (d, J_o = 8.8 Hz, 2H), 7.29 (ddd, J_o = 7.0 Hz, J_m = 1.2 Hz, 1H), 7.4 (d, J_o = 8.8 Hz, 2H), 7.52 (dd, J_o = 8.0 Hz, J_m= 1.2 Hz, 1H), 7.67 (ddd, J_o = 6.8 Hz, J_m = 1.4 Hz, 1H), 7.86 (dd, J_o = 7.8 Hz, J_m = 1.6 Hz, 1H), 10.5 ppm (s, 1H); IR (KBr): ν = 3338, 2132, 1338, 1164 cm^{-1}; MS (EI, 70 eV): *m/z*: 354/352 [M]$^+$.

2-Azido-N-(4-methoxyphenyl) benzenesulfonamide (**4e**). Brown crystals. Yield 78%; m.p.: 130 °C; ^{1}H-NMR (200 MHz, DMSO-d_6): δ = 3.63 (s, 3H), 6.76 (d, J_o = 9.3 Hz, 2H), 7.01 (d, J_o = 8.7 Hz, 2H), 7.23 (ddd, J_o = 7.4, J_m = 1.1 Hz, 1H), 7.51 (dd, J_o = 7.9 Hz, J_m = 1.1 Hz, 1H), 7.62 (ddd, J_o = 7.8 Hz, J_m = 1.6 Hz, 1H), 7.73 (dd, J_o = 7.9 Hz, J_m = 1.2 Hz, 1H), 9.87 ppm (s, 1H); IR (KBr): ν = 3274, 2138, 1336, 1164 cm^{-1}; MS (EI, 70 eV): *m/z*: 304 [M]$^+$.

Ethyl-4-(2-azidophenylsulfonamido) benzoate (**4f**). Brown crystals. Yield 78%; m.p.: 182–184 °C; ^{1}H-NMR (200 MHz, DMSO-d_6): δ = 1.23 (t, J_o = 7.0 Hz, 3H), 4.20 (q, J_o = 7.1 Hz, 2H), 7.19 (BB', J_o = 8.7 Hz, 2H), 7.30 (ddd, J_o = 7.8 Hz, 1H), 7.48 (dd, J_o = 8.1 Hz, 1H), 7.65 (ddd, J_o = 7.8 Hz, 1H), 7.77 (AA', J_o = 8.7 Hz, 2H), 7.94 (dd, J_o = 7.8 Hz, 1H), 10.9 ppm (s, 1H); IR (KBr): ν = 3230, 2110, 1690, 1300, 1165 cm^{-1}; MS (EI, 70 eV): *m/z*: 346 [M]$^+$.

3.1.5. General Procedures for Synthesizing 9-(*R*)-6,11-Dihydrodibenzo[c,f][1,2,5]thiadiazepine-5,5-dioxides **2a–f**

2-Azido-*N*-(4-(*R*)phenyl) benzenesulfonamide **4** (0.2 g, 0.73 mmol) was added to a solution of diphenyl ether (10 mL, 63 mmol) at 208 °C. The solution was stirred for 5 min then cooled to room temperature. The reaction mixture was purified by flash chromatography (70:30, ethyl acetate–hexane). The resulting residue was recrystallized in ethyl acetate–hexane (30:70). Compounds **2a** and **2d** were previously reported by Altannira *et al.* [8], and spectroscopic data are in agreement with those reported here.

6,11-Dihydrodibenzo[c,f][1,2,5]thiadiazepine-5,5-dioxide (**2a**). Brown crystals (0.50 mmol, 69%); m.p.: 198 °C; ^{1}H-NMR (300 MHz, DMSO-d_6): δ = 6.82 (ddd, J_o = 7.8 Hz, J_m = 0.9 Hz, 1H), 6.88 (dd, J_o = 7.4 Hz, J_m = 1.5 Hz, 1H), 7.03 (ddd, J_o = 7.7 Hz, J_m = 1.5 Hz, 1H), 7.07 (dd, J_o = 8.1 Hz, J_m = 1.5 Hz, 1H), 7.14 (ddd, J_o = 7.5 Hz, J_m = 1.5 Hz, 1H), 7.18 (dd, J_o = 8.2 Hz, J_m = 1.0 Hz, 1H), 7.37 (ddd, J_o = 7.7 Hz, J_m = 1.6 Hz, 1H), 7.61 (dd, J_o = 8.0 Hz, J_m = 1.6 Hz, 1H), 8.98 (s, 1H), 9.80 ppm (s, 1H); ^{13}C-NMR (75 MHz, DMSO-d_6): δ = 117.5, 119.5, 119.6, 121.1, 125.2, 125.9, 127.3, 128.4, 128.8, 132.9, 139.5, 139.9 ppm; IR (KBr): ν = 3380, 3301, 1313, 1160 cm^{-1}; MS (EI, 70 eV): *m/z*: 246 [M]$^+$; Anal. calculated for $C_{12}H_{10}N_2O_2S$: C 58.52%, H 4.09%, N 11.37%, found: C 58.11%, H 4.11%, N 11.13%.

9-Fluoro-6,11-dihydrodibenzo[c,f][1,2,5]thiadiazepine-5,5-dioxide (**2b**). Colorless needle crystals. Yield 70%; m.p.: 202 °C; ^{1}H-NMR (300 MHz, DMSO-d_6): δ = 6.69 (ddd, J_o= 8.2 Hz, J_{mH-F} = 3.0 Hz, 1H), 6.86 (dd, J_o = 7.2 Hz, 1H), 6.89 (d, J_m = 2.7 Hz, 1H), 7.05 (dd, J_o = 7.5 Hz, 1H), 7.16 (dd, J_o = 8.1 Hz, J_m = 0.6 Hz, 1H), 7.41 (ddd, J_o = 7.6 Hz, J_m = 1.5 Hz, 1H), 7.63 (dd, J_o = 8.0 Hz, J_m = 1.8 Hz, 1H), 9.14 (s, 1H), 9.78 ppm (s, 1H); ^{13}C-NMR (75 MHz, DMSO-d_6): δ = 105.6, 107.6, 119.0, 121.4, 126.1, 129.3, 130.4, 133.1, 139.2, 141.3, 159.2, 162.5 ppm; IR (KBr): ν = 3365, 3226, 1295, 1159 cm^{-1}; MS (EI, 70 eV): *m/z*: 264 [M]$^+$; Anal. calculated for $C_{12}H_9N_2O_2SF$: C 54.54%, H 3.43%, N 10.60%, found: C 54.05%, H 3.32%, N 10.34%.

9-Chloro-6,11-dihydrodibenzo[c,f][1,2,5]thiadiazepine-5,5-dioxide (**2c**). White powder. Yield 79%; m.p.: 248 °C; ^{1}H-NMR (300 MHz, DMSO-d_6): δ = 6.87 (ddd, J_o = 7.8 Hz, J_m = 1.2 Hz, 1H), 6.88 (dd, J_o = 8.4 Hz, J_m = 2.1 Hz, 1H), 7.01 (d, J_o = 8.4 Hz, 1H), 7.13 (d, J_m = 2.1 Hz, 1H), 7.15 (dd, J_o = 8.1 Hz, J_m = 0.6 Hz, 1H), 7.41 (ddd, J_o = 7.7 Hz, J_m = 1.5 Hz, 1H), 7.62 (dd, J_o = 8.0 Hz, J_m = 1.6 Hz, 1H), 9.11 (s, 1H), 9.95 ppm (s, 1H); ^{13}C-NMR (75 MHz, DMSO-D$_6$): δ = 118.3, 118.7, 119.7, 120.4, 124.2, 125.8, 129.2, 129.5, 131.1, 133.3, 139.2, 140.5 ppm; IR (KBr): ν = 3369, 3269, 1304, 1156cm^{-1}; MS (EI, 70 eV): *m/z*: 280 [M]$^+$; Anal. calculated for $C_{12}H_9N_2O_2SCl$: C 51.34%, H 3.23%, N 9.98%, found: C 51.03%, H 3.22%, N 9.81%.

9-Bromo-6,11-dihydrodibenzo[c,f][1,2,5]thiadiazepine-5,5-dioxide (**2d**). Brown powder. Yield 85%; m.p.: 250 °C; ^{1}H-NMR (300 MHz, DMSO-d_6): δ = 6.87 (ddd, J_o = 7.4 Hz, 1H), 6.94 (d, J_o = 8.4 Hz, 1H), 7.01 (dd, J_o = 8.2 Hz, J_m = 2.0 Hz, 1H), 7.15 (d, J_o = 8.4 Hz, 1H), 7.28 (d, J_m = 1.8 Hz, 1H), 7.41 (ddd, J_o = 7.8 Hz, 1H), 7.62 (dd, J_o = 7.8 Hz, J_m = 1.2 Hz, 1H), 9.10 (s, 1H), 9.96 ppm (s, 1H); ^{13}C-NMR (75 MHz, DMSO-d_6): δ = 118.3, 119.2, 119.7, 121.6, 123.3, 124.6, 125.8, 129.2, 129.7, 133.3, 139.2, 140.7 ppm; IR (KBr): ν = 3371, 3268, 1308, 1160 cm^{-1}; MS (EI, 70 eV): *m/z*: 326/324

[M]$^+$; Anal. calculated for $C_{12}H_9N_2O_2SBr$: C 44.32%, H 2.79%, N 8.61%, found: C 44.09%, H 2.81%, N 8.74%.

9-Methoxy-6,11-dihydrodibenzo[c,f][1,2,5]thiadiazepine-5,5-dioxide (**2e**). Yellow crystals. Yield 67%; m.p.: 171 °C; ^{1}H-NMR (300 MHz, DMSO-d_6): δ = 3.73 (s, 3H), 6.49 (dd, J_o = 8.7 Hz, J_m = 2.7 Hz, 1H), 6.66 (d, J_m = 2.7 Hz, 1H), 6.83 (ddd, J_o = 7.5 Hz, J_m = 0.9 Hz, 1H), 6.96 (d, J_o = 8.7 Hz, 1H), 7.17 (d, J_o = 7.8 Hz, 1H), 7.37 (ddd, J_o = 7.7 Hz, J_m = 1.5 Hz, 1H,), 7.62 (dd, J_o = 7.8 Hz, J_m = 1.5 Hz, 1H), 8.99 (s, 1H), 9.51 ppm (s, 1H); ^{13}C-NMR (75 MHz, DMSO-D_6): δ = 55.2, 104.2, 107.4, 117.7, 118.1, 119.5, 126.3, 129.0, 130.4, 132.8, 139.7, 141.2, 158.6 ppm; IR (KBr): ν = 3374, 3228, 1322, 1149 cm^{-1}; MS (EI, 70 eV): *m/z*: 276 [M]$^+$; Anal. calculated for $C_{13}H_{12}N_2O_3S$: C 56.51%, H 4.38%, N 10.14%, found: C 56.56%, H 4.40%, N 9.89%.

Ethyl 6,11-dihydrodibenzo[c,f][1,2,5]thiadiazepine-9-carboxylate-5,5-dioxide (**2f**). Brown crystals. Yield 12%; m.p.: 227 °C; ^{1}H-NMR (300 MHz, DMSO-d_6): δ = 1.31 (t, J_o = 7.0 Hz, 3H), 4.30 (q, J_o = 7.2 Hz, 2H), 6.85 (ddd, J_o = 7.5 Hz, 1H), 7.07 (d, J_o = 8.1 Hz, 1H), 7.19 (d, J_o = 7.8 Hz, 1H), 7.40 (dd, J_o = 8.1 Hz, 1H), 7.40 (ddd, J_o = 7.6 Hz, 1H), 7.61 (dd, J_o = 7.8 Hz, J_m = 1.5 Hz, 1H), 7.73 (d, J_m = 1.8 Hz, 1H), 9.20 (s, 1H), 10.3 ppm (s, 1H); ^{13}C-NMR (75 MHz, DMSO-d_6): δ = 14.2, 60.7, 118.1, 119.6, 120.4, 121.3, 125.3, 126.8, 128.2, 128.9, 129.6, 133.4, 138.3, 139.6, 165.1 ppm; IR (KBr): ν = 3360, 3234, 1700, 1328, 1170 cm^{-1}; MS (EI, 70 eV): *m/z*: 318 [M]$^+$; Anal. calculated for $C_{15}H_{14}N_2O_4S$: C 56.59%, H 4.43%, N 8.80%, found: C 56.67%, H 4.44%, N 8.64%.

3.1.6. Procedure for Synthesizing 6,11-Dihydrodibenzo[c,f][1,2,5]thiadiazepine-9-carboxylic acid 5,5-dioxide (**2g**)

A solution of potassium hydroxide 10% (w/v) was added to ethyl 6,11-dihydrodibenzo [*c,f*][1,2,5]thiadiazepine-9-carboxylate-5,5-dioxide (**2f**, 0.5 g, 1.57 mmol). The reaction mixture was heated under reflux and stirred for 60 min, after which a chloride acid solution was added to a pH of 6. The resulting solid was collected, washed with water, and dried under vacuum. The resulting yellow solid residue was obtained in a quantitative yield; m.p.: 350 °C; ^{1}H-NMR (300 MHz, DMSO-d_6): δ = 6.84 (ddd, J_o = 7.6 Hz, J_m = 1.0 Hz, 1H), 7.05 (d, J_o = 8.1 Hz, 1H), 7.18 (d, J_o = 8.1 Hz, 1H), 7.39 (dd, J_o = 8.1 Hz, J_m = 1.8 Hz, 1H), 7.39 (ddd, J_o = 7.6 Hz, J_m = 1.8 Hz, 1H), 7.61 (dd, J_o = 8.0 Hz, J_m = 1.6 Hz, 1H), 7.72 (d, J_m = 1.8 Hz, 1H), 9.15 (s, 1H), 10.7 ppm (s, 2H); ^{13}C-NMR (75 MHz, DMSO-d_6): δ = 118.0, 119.6, 120.7, 121.6, 125.4, 126.8, 128.9, 129.3, 129.4, 133.4, 138.3, 139.7, 166.7 ppm; IR (KBr): ν = 3360, 3234, 1700, 1328 cm^{-1}; MS (EI, 70 eV): *m/z*: 290 [M]$^+$; Anal. calculated for $C_{13}H_{10}N_2O_4S$: C 53.79%, H 3.47%, N 9.65%, found: C 53.73%, H 3.47%, N 9.28%.

3.2. Biological Methods

3.2.1. Primary Cultures of the Myenteric Neurons

Guinea pigs (100–200 g; either male or female) were sacrificed by cervical dislocation and carotid exsanguination. These methods have been approved by the Animal Care Committee of the IPICYT and are in agreement with the published Guiding Principles in the Care and Use of Animals, approved by the American Physiological Society. A segment of ~10 cm of the jejunum was removed and placed in

a modified Krebs solution (in mM: NaCl, 126; NaH_2PO_4, 1.2; $MgCl_2$, 1.2; $CaCl_2$, 2.5; KCl, 5; NaH_2CO_3, 25; glucose, 11. The sample was gassed under 95% O_2 and 5% CO_2) and opened longitudinally. A dissecting microscope was used to dissect the mucosa and submucosa layers prior to removing most of the circular muscle layer, leaving the myenteric plexus embedded in a longitudinal layer.

The cell isolation procedure has been described elsewhere [26]. The myenteric preparation was dissociated by sequential treatment with two enzymatic solutions: the first solution contained papain (0.01 $mL \cdot mL^{-1}$ activated with 0.4 $mg \cdot mL^{-1}$ L-cysteine), and the second solution contained collagenase (1 $mg \cdot mL^{-1}$) and dispase (4 $mg \cdot mL^{-1}$). The enzymes were removed by washing the neurons with L15 medium, and the neurons were placed on round coverslips coated with sterile rat-tail collagen. The culture medium was varied from minimal medium to essential medium 97.5% containing 2.5% guinea pig serum, 2 mM L-glutamine, 10 $U \cdot mL^{-1}$ penicillin, 10 $\mu g \cdot mL^{-1}$ streptomycin, and 15 mM glucose.

3.2.2. Whole-Cell Recordings of the Membrane Currents Induced by GABA

To reduce the effects of the membrane currents other than those mediated by the activation of LGIC, experiments were conducted in the presence of Cs^+ (a potassium channel blocker). This was important because GABA modulates the membrane ion channels of the central neurons (enteric neurons) via G-protein linked receptors [27–29]. Membrane currents induced by GABA were recorded using a Gene Clamp 500B amplifier (Molecular Devices, CA, USA). The holding potential was −60 mV (unless otherwise stated), and the short-term (4–50 h) primary cultures of the myenteric neurons were used to prevent space-clamp problems due to neurite growth. Glass pipettes with a resistance of 2–5 MΩ were prepared as described previously [25]. This low resistance and slight suction inside the pipette during the recordings maintained a low series resistance (around 6 MΩ).

All experiments were conducted using standard solutions with the following compositions (in mM); inside the pipette: CsCl, 160; EGTA, 10; HEPES, 5; NaCl, 10; ATPMg, 3 and GTP, 0.1; external solution: NaCl, 160; $CaCl_2$, 2; glucose, 11; HEPES, 5 and CsCl, 3. The pH of all solutions was adjusted to 7.3–7.4 using either CsOH (pipette solution) or NaOH (external solution). The seal resistance in the whole-cell mode ranged from 1 to 10 GΩ. The whole-cell current data were recorded on a PC using the AxoScope software (Axon Instruments, Inc.) and were analyzed using the AXOGRAPH software (Molecular Devices, CA, USA). The recording chamber was superfused with an external solution at ~2 $mL \cdot min^{-1}$. The solution around the neuron was quickly exchanged during recordings using an eight-tube device. Each tube was connected to a syringe (10 mL) containing either the control or the experimental solution. A control tube was positioned ~300 μm in front of the recorded neuron, and substances were applied externally by abruptly interchanging the tube for another tube containing the control solution plus the drug(s). Desensitization of the $GABA_A$ receptors was prevented by applying GABA at intervals of at least 5 min, in between cells were continuously superfused with extracellular solution. Experimental substances were removed by returning to the control solution. External solutions were applied by gravity, and the height of the syringes was continuously adjusted to minimize changes in the flow rate. The experiments were performed at room temperature (24 ± 1 °C).

3.2.3. Solutions and Reagents

L15 medium, minimum essential medium, Hanks solution, penicillin-streptomycin, and L-glutamine were purchased from GIBCO (Life Technologies Corp., Carlsbad, CA, USA). Collagenase and papain were purchased from Worthington (Worthington Biochemical Corp., Lakewood, NJ, USA), and dispase was purchased from Roche (Indianapolis, IN, USA). Cesium chloride, sodium chloride, ethylene glycol-bis(2-aminoethylether)-*N,N,N',N'*-tetra-acetic acid (EGTA), HEPES, adenosine-5'-triphosphate magnesium salt (ATP magnesium salt), guanosine-5'-triphosphate sodium salt (GTP sodium salt), cesium hydroxide, flumazenil, GABA, picrotoxin, and dimethyl sulfoxide were purchased from Sigma-Aldrich (St. Louis, MO, USA). Pentobarbital-Na was purchased from Lab Ttokkyo, S.A. (México, D.F., Mexico). Stock solutions (0.01–1 M) were prepared using de-ionized distilled water and were stored frozen, except for picrotoxin and the DBTD stock solutions, which were prepared in ethanol (50% v/v) and DMSO, respectively. The desired final drug concentration was obtained by diluting the stock solutions in an external solution prior to application.

3.2.4. Data Analysis

The concentration–response data were fit to a logistic model:

$$I = I_{max}/[1 + (EC_{50}/[A])^{nH}] \quad (1)$$

where [A] is the agonist concentration, I is the current, and I_{max} is the maximum current. EC_{50} is the concentration of drug that elicits a half-maximum response, and nH is the Hill coefficient. Experimental data were reported as ± SEM, and n represents the number of cells used. The unpaired Student's t-test was applied to data obtained from two different groups of cells. One-way ANOVA and the Bonferroni tests were used to compare multiple means. The two-tailed *P* values of 0.05 or less were considered to be statistically significant.

3.2.5. Theoretical Calculations

Quantum chemical calculations of the DBTDs structures **2a–g** in the gas phase were performed using GAUSSIAN 03 [30] in conjunction with density functional theory (DFT) calculations. Geometry optimization of the DBTDs was followed by frequency calculations performed at the B3LYP/6-311 ++G(d,p) level. Table 1 reports the cLog *P*, generated using HyperChem, of each optimized structure obtained from Gaussian V03.

4. Conclusions

We described the preparation of novel DBTDs via a nitrene radical that inserted into the C on the aromatic ring. Seven derivatives **2a–g** were generated and their effects on $GABA_A$ neuronal receptors were tested. It was shown, for the first time, that DBTDs inhibited I_{GABA} in a time- and concentration-dependent manner.

The DBTDs displayed an inhibitory effect on the $GABA_A$ channel of myenteric neurons, and this antagonism was non-competitive indicating that it does not bind to the GABA receptor and their effect is likely allosteric. Inhibition was mediated by an extracellular binding site that was most likely not in

the mouth of the channel and therefore, it is unlikely that this effect is mediated by channel blockage. Their effect was also independent of the benzodiazepine binding site. The DBTDs described here could be used as a model to explore new $GABA_A$ receptor inhibitors with a potential to be used as antidotes for substances known to positively modulate $GABA_A$ channel activity or as a new drugs to induce experimental epilepsy. These compounds appear to bind on a different site than picrotoxin; therefore, they could be used alone or in combination with picrotoxin. Future experiments will be aimed to molecularly identify DBTDs binding sites on $GABA_A$ receptors.

Acknowledgments

The authors wish to thank Estela Nuñez-Pastrana and María Guadalupe Ortega-Salazar (Facultad de Ciencias Químicas, UASLP) for their technical assistance. This work was supported by CONACYT, México (Project no. 134687). Support for this work by the UASLP via FAI (C03-FAI-11-21.56) and PIFI 2.0 is gratefully acknowledged. We also thank A. Peña, E. Huerta, E. Hernández, L. Velasco, and J. Pérez from the Instituto de Química (UNAM) for technical support. J.F. Ramírez Martínez was supported by a CONACYT scholarship (181001).

Conflict of Interest

The authors declare no conflict of interest.

References

1. Weber, A. 5,5-dioxodibenzo[1,2,5]-thiadiazepines and intermediates therefor. U.S. Patent 3268557, 1966.
2. Weber, A.; Frossard, J. Research on tricyclic psychotropic drugs. Dibenzothiadizepines. *Ann. Pharm. Fr.* **1966**, *24*, 445–450.
3. Weber, A. 5,5-dioxodibenzo[1,2,5]thiadiazepines derivatives and method of use. U.S. Patent 3274058, 1966.
4. Giannotti, D.; Viti, G.; Sbraci, P.; Pestellini, V.; Volterra, G.; Borsini, F.; Lecci, A.; Meli, A.; Dapporto, P.; Paoli, P. New dibenzothiadiazepine derivatives with antidepressant activities. *J. Med. Chem.* **1991**, *34*, 1356–1362.
5. Bellarosa, D.; Antonelli, G.; Bambacioni, F.; Giannotti, D.; Viti, G.; Nannicini, R.; Giachetti, A.; Dianzani, F.; Witvrouw, M.; Pauwels, R.; *et al.* New arylpyrido-diazepine and -thiodiazepine derivatives are potent and highly selective HIV-1 inhibitors targeted at the reverse transcriptase. *Antiviral. Res.* **1996**, *30*, 109–124.
6. Silvestri, R.; Marfe, G.; Artico, M.; La Regina, G.; Lavecchia, A.; Novellino, E.; Morgante, E.; Di Stefano, C.; Catalano, G.; Filomeni, G.; *et al.* Pyrrolo[1,2-b][1,2,5]benzothiadiazepines (PBTDs): A new class of agents with high apoptotic activity in chronic myelogenous leukemia K562 cells and in cells from patients at onset and who were imatinib-resistant. *J. Med. Chem.* **2006**, *49*, 5840–5844.
7. Goldberg, I. Ueber Phenylirungen bei Gegenwart von Kupfer als Katalysator. *Ber. Dtsch. Chem. Ges.* **1906**, *39*, 1691–1692.

8. Altamura, M.; Fedi, V.; Giannotti, D.; Paoli, P.; Rossi, P. Privileged structures: Synthesis and structural investigations on tricyclic sulfonamides. *New J. Chem.* **2009**, *33*, 2219–2231.
9. Jian, H.H.; Tour, J.M. En route to surface-bound electric field-driven molecular motors. *J. Org. Chem.* **2003**, 68, 5091–5103.
10. Tsao, M.L.; Gritsan, N.; James, T.R.; Platz, M.S.; Hrovat, D.A.; Borden, W.T. Study of the chemistry of ortho- and para-biphenylnitrenes by laser flash photolysis and time-resolved IR experiments and by B3LYP and CASPT2 calculations. *J. Am. Chem. Soc.* **2003**, *125*, 9343–9358.
11. Shou, W.G.; Li, J.A.; Guo, T.X.; Lin, Z.Y.; Jia, G.C. Ruthenium-Catalyzed Intramolecular Amination Reactions of Aryl- and Vinylazides. *Organometallics* **2009**, *28*, 6847–6854.
12. Stokes, B.J.; Jovanovic, B.; Dong, H.J.; Richert, K.J.; Riell, R.D.; Driver, T.G. Rh-2(II)-Catalyzed Synthesis of Carbazoles from Biaryl Azides. *J. Org. Chem.* **2009**, *74*, 3225–3228.
13. Cherney, R.J.; Duan, J.J.W.; Voss, M.E.; Chen, L.H.; Wang, L.; Meyer, D.T.; Wasserman, Z.R.; Hardman, K.D.; Liu, R.Q.; Covington, M.B.; *et al.* Design, synthesis, and evaluation of benzothiadiazepine hydroxamates as selective tumor necrosis factor-alpha converting enzyme inhibitors. *J. Med. Chem.* **2003**, *46*, 1811–1823.
14. Giannotti, D.; Viti, G.; Nannicini, R.; Pestellini, V.; Bellarosa, D. *Bioorg. Med. Chem. Lett.* **1995**, *5*, 1461–1466.
15. Enna, S.J. The GABA Receptors. In *The Receptors*; Enna, S.J., Mohler, H., Eds.; Humana Press Inc.: Totowa, NJ, USA, 2012.
16. Krystal, J.H.; Sanacora, G.; Blumberg, H.; Anand, A.; Charney, D.S.; Marek, G.; Epperson, C.N.; Goddard, A.; Mason, G.F. Glutamate and GABA systems as targets for novel antidepressant and mood-stabilizing treatments. *Mol. Psychiatr.* **2002**, *7*, S71–S80.
17. Brickley, S.G.; Mody, I. Extrasynaptic GABA(A) receptors: Their function in the CNS and implications for disease. *Neuron* **2012**, *73*, 23–34.
18. Zhou, X.; Galligan, J.J. GABA(A) receptors on calbindin-immunoreactive myenteric neurons of guinea pig intestine. *J. Auton. Nerv. Syst.* **2000**, *78*, 122–135.
19. Karanjia, R.; Garcia-Hernandez, L.M.; Miranda-Morales, M.; Somani, N.; Espinosa-Luna, R.; Montano, L.M.; Barajas-Lopez, C. Cross-inhibitory interactions between GABAA and P2X channels in myenteric neurones. *Eur. J. Neurosci.* **2006**, *23*, 3259–3268.
20. Miranda-Morales, M.; Garcia-Hernandez, L.M.; Ochoa-Cortes, F.; Espinosa-Luna, R.; Naranjo-Rodriguez, E.B.; Barajas-Lopez, C. Cross-talking between 5-HT3 and GABAA receptors in cultured myenteric neurons. *Synapse* **2007**, *61*, 732–740.
21. Krehan, D.; Storustovu, S.I.; Liljefors, T.; Ebert, B.; Nielsen, B.; Krogsgaard-Larsen, P.; Frolund, B. Potent 4-arylalkyl-substituted 3-isothiazolol GABA(A) competitive/noncompetitive antagonists: synthesis and pharmacology. *J. Med. Chem.* **2006**, *49*, 1388–1396.
22. Kenakin, R. *Pharmacologic Analysis of Drug–Receptor Interaction*, 2nd ed.; Raven Press Ltd.: New York, NY, USA, 1993.
23. Olsen, R.W. Picrotoxin-like channel blockers of GABAA receptors. *Proc. Natl. Acad. Sci. USA* **2006**, *103*, 6081–6082.
24. Sieghart, W.; Ramerstorfer, J.; Sarto-Jackson, I.; Varagic, Z.; Ernst, M. A novel GABAA receptor pharmacology: Drugs interacting with the a(+) b(-) interface. *Br. J. Pharmacol.* **2012**, *166*, 476–485.

25. Saeed, A.; Rama, N.H. Synthesis of some new 2-Aryl-2,3-dihydro-1,2,3-benzothiadiazol-1,1-dioxides. *J. Chem. Soc. Pak.* **1997**, *19*, 236–239.
26. Barajas-Lopez, C.; Peres, A.L.; Espinosa-Luna, R. Cellular mechanisms underlying adenosine actions on cholinergic transmission in enteric neurons. *Am. J. Physiol.* **1996**, *271*, C264–C275.
27. Wellendorph, P.; Brauner-Osborne, H. Molecular basis for amino acid sensing by family C G-protein-coupled receptors. *Br. J. Pharmacol.* **2009**, *156*, 869–884.
28. Cherubini, E.; North, R.A. Actions of gamma-aminobutyric acid on neurones of guinea-pig myenteric plexus. *Br. J. Pharmacol.* **1984**, *82*, 93–100.
29. Krantis, A. GABA in the Mammalian Enteric Nervous System. *News Physiol. Sci.* **2000**, *15*, 284–290.
30. Frisch, G.W.T.M.J.; Schlegel, H.B.; Scuseria, G.E.; Robb, M.A.; Cheeseman, J.R.; Montgomery, J.A.; Vreven, .T.; Kudin, K.N.; Burant, J.C.; Millam, J.M.; *et al. Gaussian v03*; Gaussian, Inc.: Wallingford, CT, USA, 2004.

Sample Availability: Contact the corresponding authors.

APPENDIX B

European Journal of Pharmacology 626 (2010) 179–185

Contents lists available at ScienceDirect

European Journal of Pharmacology

journal homepage: www.elsevier.com/locate/ejphar

Molecular and Cellular Pharmacology

Two suramin binding sites are present in guinea pig but only one in murine native P2X myenteric receptors

Raquel Guerrero-Alba [a], Eduardo Valdez-Morales [a], Esri H. Juárez [a], Marcela Miranda-Morales [a], Juan F. Ramírez-Martínez [a], Rosa Espinosa-Luna [a], Carlos Barajas-López [a,b,*]

[a] División de Biología Molecular, Instituto Potosino de Investigación Científica y Tecnológica, San Luis Potosí, SLP, Mexico
[b] Department of Anatomy and Cell Biology, Queen's University, Kingston, Ontario, Canada

ARTICLE INFO

Article history:
Received 14 July 2009
Received in revised form 8 September 2009
Accepted 28 September 2009
Available online 8 October 2009

Keywords:
Myenteric neuron
P2X receptor
Enteric neuron
Gastrointestinal tract
ATP
Suramin
PPADS
(mouse)
(guinea pig)

ABSTRACT

Whole-cell patch clamp recordings were used to characterise the physiological and pharmacological properties of P2X receptors of mouse and guinea pig myenteric neurons from the small intestine. ATP application induced a rapid inward current in 95% of recorded neurons of both species when were voltage clamped at −60 mV. Concentration–response curves for ATP (1–3000 μM) yielded EC_{50} values of 114 and 115 μM for mouse and guinea pig myenteric neurons, respectively, with a Hill coefficient value of 1.02 and 0.79, respectively, which were not significantly different of unity. α,β-methylene ATP (100 μM) was virtually inactive in both species. Pyridoxalphophate-6-azophenyl-2′,4′-disulphonic acid (0.01–30 μM) inhibited the ATP-induced currents (I_{ATP}) with a different potency; being the IC_{50} 0.6 and 1.8 μM in mouse and guinea pig, respectively. In mouse myenteric neurons, I_{ATP} were inhibited by suramin whereas in guinea pig neurons we observed two effects, potentiation and inhibition of these currents. On guinea pig, both effects of suramin had different recovering kinetics and concentration dependency, indicating that they are mediated by at least two different binding sites. Our observations indicate that myenteric P2X receptors in these two species have different pharmacological properties.

1. Introduction

P2X receptors are a family of ionotropic cation channels, activated by extracellular adenosine 5′-triphosphate (ATP). To date, seven P2X subunits have been cloned ($P2X_{1-7}$), and the subunits may assemble as trimers to form functional P2X receptors (Torres et al., 1999). All P2X subunits, except P2X6, have been reported to form functional homomeric receptors and all of them can combine with others to form heteromeric functional receptors with an unknown stoichiometry but with specific biophysical and pharmacological properties (Bo et al., 1995; Brake et al., 1994; Chen et al., 1995; Surprenant et al., 1995; Valera et al., 1994). These properties, defined in heterologous expression systems, are helpful to propose putative subunit combinations of P2X native receptors of a given tissue. However, pharmacological profiles of these recombinant P2X receptors do not always match those of the endogenous P2X receptors, thus it is plausible that some native receptors are hetero-multimeric channels composed of different P2X subunits or different subtypes of subunits produced by alternative splicing (Evans et al., 1995; North, 2002).

Experimental evidence for the existence of at least three different P2X subunits has been found in myenteric neurons of the guinea pig small intestine. Thus, immunoreactivity has been shown for $P2X_2$ (Castelucci et al., 2002), $P2X_3$, (Poole et al., 2002; Van Nassauw et al., 2002) and $P2X_7$ subunits (Hu et al., 2001). In murine myenteric neurons, immunoreactivity for $P2X_2$ (Ren et al., 2003), $P2X_3$ and $P2X_5$ (Ruan and Burnstock, 2005) has been demonstrated. Lack of inmunoreactivity for $P2X_1$, $P2X_4$ nor $P2X_6$ subunits has been reported in mouse (Ruan and Burnstock, 2005) and guinea pig (Hu et al., 2001) myenteric neurons.

There are controversial findings regarding the pharmacological properties of myenteric P2X receptors, which could reflect the existence of different receptor subtypes and interspecies differences. For instance, suramin, an antagonist for many P2X receptors was reported to potentiate (Barajas-Lopez et al., 1993, 1996a), to inhibit (Galligan and Bertrand, 1994), or have not effect (Glushakow et al., 1998) on responses mediated by myenteric P2X receptors of guinea pig small intestine. A more recent study, reports that suramin can both potentiate and inhibit these receptors in these neurons (Hu et al., 2001). In rat myenteric neurons, the inhibitory effect of suramin on P2X receptors has been the only described effect (Ohta et al., 2005). Therefore, we carried out a comparative study in murine and guinea pig

Abbreviations: α,β-meATP, α,β-methylene ATP; I_{ATP}, ATP-induced currents; PPADS, Pyridoxalphophate-6-azophenyl-2′,4′-disulphonic acid.

* Corresponding author. Instituto Potosino de Investigación Científica y Tecnológica (IPICYT), Camino a la Presa San José 2055, Col. Lomas 4a Sección, SLP, SLP, CP78216, Mexico. Tel.: +52 444 834 2000x2033; fax: +52 444 834 2010.
E-mail address: cbarajas@ipicyt.edu.mx (C. Barajas-López).

0014-2999/$ – see front matter © 2009 Elsevier B.V. All rights reserved.
doi:10.1016/j.ejphar.2009.09.063